Zootaxa 5768 (1): 001–028
https://www.mapress.com/zt/

Article

ISSN 1175-5326 (print edition)
ZOOTAXA
ISSN 1175-5334 (online edition)

https://doi.org/10.11646/zootaxa.5768.1.1
http://zoobank.org/urn:lsid:zoobank.org:pub:BDE31A16-C480-4040-B552-C4B91CB076F1

Description of a new species of African pipistrelle-like bat (Chiroptera: Vespertilionidae: *Afronycteris*)

TERESA KEARNEY[1,2,*], MARINDA DE VRIES[3] & WANDA MARKOTTER[3]
[1]*Ditsong National Museum of Natural History, PO Box 413, Pretoria, 0001, South Africa*
[2]*Department of Zoology and Entomology, University of Pretoria, Private Bag 20, Pretoria, 0028, South Africa*
[3]*Centre for Viral Zoonoses, Department of Medical Virology, University of Pretoria, Pretoria, 0002, South Africa*
marinda.devries@up.ac.za; https://orcid.org/0000-0001-9286-1040
wanda.markotter@up.ac.za; https://orcid.org/0000-0002-7550-0080
**Corresponding author: kearney@Ditsong.org.za; https://orcid.org/0000-0002-0050-4060*

Abstract

The taxonomy of the small, sub-Saharan, insectivorous bat, *Afronycteris helios* (Heller, 1912), has been unresolved for decades. The name *A*. cf. *helios* was introduced in the literature to recognise bats found in east and southern Africa that were like *A. helios* but had glands on the uropatagium. Cranio-dental morphology, bacular morphology, and molecular genetics (albeit the latter two being without representation of *A. helios*), provided evidence to formally describe "*A*. cf. *helios*", which is currently known from Kenya, Mozambique, and South Africa. Bayesian analyses based on cytochrome oxidase b, cytochrome c oxidase subunit 1, and 12S rRNA confirm that it belongs to the genus *Afronycteris* with *A. nanus* (Peter, 1852) and *A. helios*. These analyses also revealed genetic, bacular, and cranio-dental morphological differences within *A. nanus*, which are described here. Pending a more thorough geographic analysis, including all existing synonyms, *A.* cf. *nanus* has been introduced to refer to bats that were smaller than *A. nanus*. Although co-occurring in north-eastern parts of South Africa, *A.* cf. *nanus* has a more westerly distribution extending to west Africa, relative to the more easterly distribution of *A. nanus*. *Afronycteris* **sp. nov.** showed at least a 6.9%, 3.4% and 2.9% nucleotide difference to its nearest relative based on cytochrome oxidase b, cytochrome c oxidase subunit 1, and 12S rRNA respectively. It is cranio-dentally smaller than *A. helios*, slightly smaller than *A. nanus*, and larger than *A.* cf. *nanus*, with a distinct baculum, and a unique pair of glands on the uropatagium.

Key words: molecular genetics, taxonomy, morphology, *Afronycteris nanus*, *Afronycteris helios*, Kruger National Park

Introduction

A revision of pipistrelle-like bats by Monadjem *et al*. (2021) provided a much-needed update of the systematic relationship for bats from sub-Saharan African and Madagascar in the tribes Vespertilionini and Pipistrellini. Based on genetic and morphological sampling Monadjem *et al*. (2021) resolved three genera in Pipistrellini, and six genera in Vespertilionini, two of which are new. *Afronycteris* was included in the newly proposed endemic African subtribe, Laephotina, which also included *Laephotis*, *Neoromicia* and *Pseudoromicia* (Monadjem *et al*., 2021). Demos *et al*. (2025) used nuclear introns and confirmed the monophyly of the new subtribe, Laephotina, and genus, *Afronycteris,* which Monadjem *et al*. (2021) had based on mitochondrial DNA. Albeit Monadjem *et al*. (2021) and Demos *et al*. (2025) having identified the sister relationship of *Laephotis* and *Neoromicia* were unable to confirm the sister relationship of *Afronycteris* with *Pseudoromicia*. *Afronycteris* was created for the genetically and morphologically distinct *Afronycteris nanus* (Peters, 1852) (Monadjem *et al*., 2021). Including the lesser known *Afronycteris helios* (Heller, 1912) in this new genus, Monadjem *et al*. (2021) pointing out that while there were sequence differences based on cytochrome oxidase b (Cytb) within the clade identified as *A*. *nanus*, they were not sure if this included *A*. *helios* and noted the relationship between these species required further study. The sequence differences within *A. nanus* (Monadjem *et al*., 2021) were not surprising given the extensive range of specimens from across sub-Saharan Africa (ACR, 2024). These differences have also been documented when sequences from

Accepted by P. Velazco: 20 Jan. 2026; published: 9 Mar. 2026

regional studies were assessed with available sequences from other regions. Prior to the recognition by Monadjem (*et al*., 2021) of *Afronycteris* for *A. nanus*, Monadjem *et al*. (2013) investigated Vespertilionidae bats occurring on Mount Nimba, which straddles Liberia, Guinea, and Cote d'Ivoire, and recorded the largest intraspecific variation, using the cytochrome c oxidase subunit 1 (COI) gene, between *Neoromicia nana* from Liberia and Cote d'Ivoire. Reporting on bats from Zambia Benda *et al*. (2022) resolved a similar phylogenetic pattern for *A. nanus* from west, east, and southern Africa based on cytochrome *b* to that in Monadjem *et al*. (2021). In a study primarily on specimens from Equatorial Guinea, Torrent *et al*. (2025) using Cytb and COI markers also showed deep sequence divergence between west and east African *A. nanus*. The numerous synonyms for *A. nanus* and the history of name changes are collated in the African Chiroptera Report (2024).

Heller (1912) described *A. helios* from northern Kenya as being most closely related to *A. nanus* albeit smaller in size and paler. The African Chiroptera report (ACR, 2024) records all the subsequent taxonomic changes to *A. helios*. Notably it was synonymised with *A. nanus* by Meester *et al*. (1986) and Koopman (1993), although, based on differences in the baculum of three individuals from Kenya, Hill and Harrison (1987) suggested *A. helios* was a species distinct from *A. nanus*. Reporting on social organisation and population dynamics of *A. nanus* in Malawi, Happold and Happold (1996) compared their results with studies purportedly on the same species from South Africa (LaVal and LaVal, 1977) and Kenya (O'Shea, 1980). In contrast to *A. nanus* being more commonly associated with musaceous plants, roosting in their rolled leaves, in the Kenyan study the bats had roosted in *Phoenix reclinate* palm fronds, both in palm trees and leaves used as roofing material. O'Shea (1980) considered whether he had used the correct taxonomy for the Kenyan bats in view of their different roost types and the presence of paired glands on either side of the uropatagium, a character not previously reported in *A. nanus*. Considering the possibility that individuals previously identified as *A. nanus* might represent different species, Happold and Happold (1996) included a personal communication with T.J. O'Shea. Based on observations of both forms (thatch roosting with glands on the uropatagium, and leaf roosting without glands on the uropatagium) that occurred together in Ivory Coast, O'Shea again suggested they might be different species. Rosevear (1965) had previously reported *A. nanus* in west Africa roosting in thatch or under rafters. La Val and La Val (1977) reported a maternity colony of 150 individuals of *A. nanus* roosting tightly grouped together in a thatch roof in the Kruger National Park, although they gave no further detail of the location of the roost or if any specimens were deposited in collections. Considering these differences, Simmons (2005) recognised *A. helios* as a distinct species. Happold and Van Cakenberghe (2013) then referred bats with glands on the uropatagium and myotodont lower molars to *A*. cf. *helios* pending further taxonomic resolution, given D. Wilson (pers. comm.) reported the holotype of *A. helios* from Kenya did not have glands on the uropatagium, or myotodont lower molars.

Revisiting bat species occurring in the northern part of the Kruger National Park, South Africa 17 years after the previous extensive work done in the area (see Rautenbach *et al*., 1985; Rautenbach *et al*., 1996, and references therein), the authors found some individuals identified in the field as *A. nanus* had glands on the uropatagium, whereas others did not. Here we present morphological and genetic data collected to enable identification of the bats that were caught in the northern part of the Kruger National Park, which were like *A. nanus* but had glands on the uropatagium, and which we describe as a new species that was previously referred to as *A*. cf. *helios*.

Materials and methods

Specimens

Bats that were caught in February and November 2010 in the Makuleka Contract Park (previously referred to as Pafuri) in the northern part of Kruger National Park (permit RB/2010/22) were deposited in the DITSONG: National Museum of Natural History (TM) and Skukuza Biological Reference Collection (CHIR-KNP) (Appendix 1 and Figure 1). The study was approved by the University of Pretoria's Animal Ethics Committee under EC059-14 and Section 20 approval from the South African Department of Agriculture, Land Reform and Rural Development (12/11/1/1/8). Additional comparative material was used from those as well as the following collections: Amathole Museum, Qonce (AM); Durban Natural Science Museum, Durban (DM); Harrison Institute, Sevenoaks (HZM); Museum für Naturkunde, Berlin (ZMB); Natural History Museum, London (NHMUK); Livingstone Museum, Livingstone (NMZL); Naturmuseum Senckenberg, Frankfurt (SMF); National Museum of Natural History, Smithsonian Institution, Washington (USNM) (Appendix 1 and Figure 1).

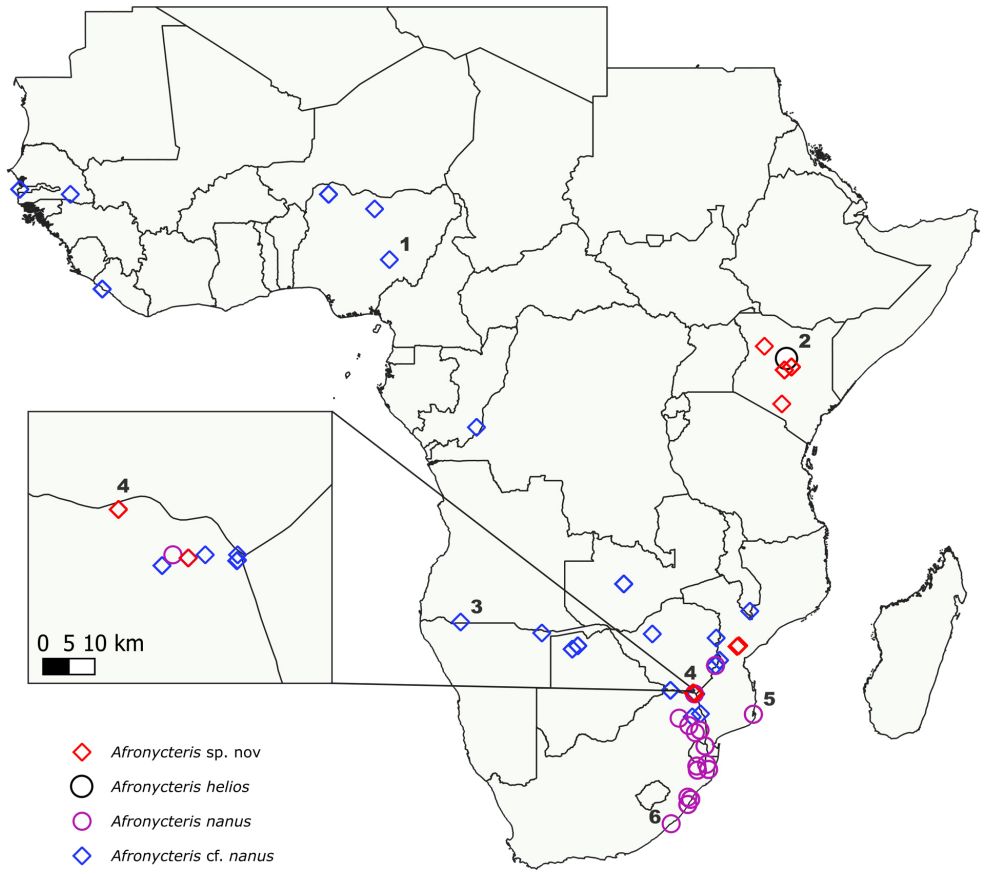

FIGURE 1. Map of localities in Africa for specimens of *Afronycteris* spp. used in the analyses of skull, bacular, external morphology, and for new sequences generated in this study (see Appendix 1). The inset indicates specimen localities in the Makuleka Contract Park in the northern part of South Africa. Numbers indicate holotypes / syntypes: 1 = *Pipistrellus culex* Thomas, 1911 (NHMUK 1911.3.24.4), 2 = *Pipistrellus helios* Heller, 1912 (USNM 181813), 3 = *Pipistrellus fouriei* Thomas, 1926 (NHMUK 1925.12.4.20), 4 = *Afronycteris rautenbachi* **sp. nov.** (TM 48535), 5 = *Vespertilio nanus* Peters, 1852 (ZMB 588a and ZMB 588c), 6 = *Pipistrellus nanus australis* Roberts 1913 (TM 1076).

Type material

The following type specimens were examined by one of the authors (TK): *Vespertilio nanus* Peters, 1852 [ZMB 588a (Syntype), ZMB 588c (Syntype)] (currently synonymised under *A. nanus*). *Pipistrellus culex* Thomas, 1911 [NHMUK 1911.3.24.4 (Holotype)] (currently synonymised under *A. nanus*). *Pipistrellus nanus australis* Roberts 1913 [TM 1076 (Holotype)], and *Pipistrellus fouriei* Thomas, 1926 [NHMUK 1925.12.4.20 (Holotype)] (currently synonymised under *A. nanus*) (Appendix 1 and Figure 1). Don Wilson examined the type of *Pipistrellus helios* Heller, 1912 [USNM 181813 (Holotype)] (Curator Emeritus, Mammals, Smithsonian Museum of Natural History, personal communication, 2011) (Appendix 1 and Figure 1).

Genetic study

Three genome regions were selected, Cytb, 12S rRNA (12S), and cytochrome c oxidase subunit 1 (COI), to investigate the genetic variation of *Afronycteris* specimens collected in the northern part of South Africa. Fifteen Cytb (GenBank accession numbers PX103059–PX103073), 15 12S (GenBank accession numbers PX105500–PX105514), and five COI sequences (GenBank accession numbers PX103240–PX103244) were generated in this study (Appendix 1). Available sample material (wing biopsy, pectoral muscle, heart, kidney or liver) was subjected to DNA extraction using the Quick-DNA™ Miniprep Plus Kit (Zymo Research, USA) according to the manufacturer's instructions. Three PCR reactions, targeting the three different regions, were prepared for each of the specimens.

For the Cytb reaction, a master mix was prepared by mixing 0.4 µM LGL-765 Forward primer, 0.4µM LGL-766 Reverse primer (Metabion, Germany) (Bickham *et al*. 1995, 2004), 0.2 mM dNTP mix (Thermo Scientific, South

Africa), 1 mM $MgCl_2$ (Thermo Scientific, South Africa), 1x DreamTaq buffer (Thermo Scientific, South Africa), 1.25U DreamTaq polymerase (Thermo Scientific, South Africa) and nuclease-free water (Ambion) to a final volume of 45 µl. To this mix, 5 µl of DNA was added and the reaction incubated at 94°C for 2 min; 45 cycles of 94°C for 30 seconds, 55°C for 30 seconds, 72°C for 90 seconds; then 72°C for 10 minutes in a SimplyAmp thermal cycler (Thermo Scientific, South Africa).

Analyses of the 12S region involved preparing a master mix of 1x DreamTaq buffer (Thermo Scientific, South Africa), 0.2 mM dNTP mix (Thermo Scientific, South Africa), 0.75 mM $MgCl_2$ (Thermo Scientific, South Africa), 0.4 µM each of the 12S-L2226M1 forward and 12S-U1230M2-CH reverse primers (Metabion, Germany) (Hassanin *et al*., 2012; Hassanin *et al*., 2017), 1.25U DreamTaq polymerase (Thermo Scientific, South Africa) and nuclease-free water (Ambion) to a final volume of 45 µl. A volume of 5 µl of sample DNA was added to the master mix, with amplification performed in a SimplyAmp thermal cycler (Thermo Scientific, South Africa) with cycling conditions set as 94°C for 4 min; 5 cycles of 94°C for 45 seconds, 60°C for 60 seconds, 72°C for 60 seconds; 30 cycles of 94°C for 30 seconds, 48°C for 45 seconds, 72°C for 60 seconds; then 72°C for 10 minutes.

For the COI gene amplification, a master mix was prepared as described for the 12S region using the Folmer-LCO1490 forward and Folmer-HCO2198 reverse primers (Metabion, Germany) (Folmer *et al*. 1994). Following the addition of the 5 µl of sample DNA, the reaction was incubated at 94°C for 2 min; 45 cycles of 94°C for 30 seconds, 48°C for 50 seconds, 72°C for 90 seconds; 72°C for 10 minutes in a SimplyAmp thermal cycler (Thermo Scientific, South Africa).

Reactions were analysed on a 1.5% agarose gel, DNA amplicons excised and purified using the Zymoclean™ Gel DNA Recovery Kit (Zymo Research. USA) according to the manufacturer's instructions. Purified DNA was subsequently subjected to Sanger sequencing and consensus sequences were generated for comparative analyses with previously published bat sequences available on the NCBI GenBank and BOLD databases. An additional 70 Cytb, 50 12S and 33 COI sequences for *Afronycteris* from other localities in Africa, as well as a diversity of Vespertilionidae (mostly Vespertilionini), including species closely related to *Afronycteris* (Monadjem *et al*., 2021) were downloaded from the GenBank database.

Sequence analysis

Multiple alignments of the nucleotide sequences of the different gene regions were generated using the ClustalW function of the BioEdit sequence alignment software v.7.2.5 (Hall, 1999). The targeted amplicon regions as per the protocols for amplified region size and edited/trimmed sequence size were: Cytb ~1140 nt and 938 nt, COI ~600-700 nt and 618 nt, and 12S ~900 nt and 872 nt. The sequence length edited per individual sample was variable based on the quality of the 5' and 3' ends of each. However, following sequence alignments, all were trimmed to the overlapping length of sequences available in the literature for comparative analyses. All were thus of equal length for the analyses as indicated above. The best-fit DNA substitution model was determined with the use of jModelTest2 (Darriba *et al*., 2012) and Bayesian phylogenies were constructed using BEAST v2.6.6 on the CIPRES Science gateway (Miller *et al*., 2010; available online at www.phylo.org/portal2/login!input.action) for each of the three alignments. The trees were run for 50 million MCMC (Markov Chain Monte Carlo) sampling every 2000 trees. Convergence was determined through visual inspection using the Tracer v1.2 software (Drummond & Rambaut, 2007). The final phylogenetic trees were constructed using TreeAnnotator (part of the BEAST package) with a burn-in of 20%. The trees were visualized in FigTree v1.4.2 and further labelled using the Inkscape software (retrieved from https://inkscape.org). Finally, *p*-distances were determined using alignments using the Molecular Evolutionary Genetics Analysis (MEGA X) software (Kumar *et al*. 2018).

Bacular study

Images and five measurements following Goodman *et al*. (2017) were taken of 19 bacula (Appendix 1): greatest overall length, greatest width of the tip and the base width, width of the shaft at its midpoint, and tip length. These were from bacula reported in Kearney *et al*. (2002), and following the methodology in Kearney *et al*. (2002), bacula that were extracted and prepared from bats caught in the Kruger National Park, and specimens in the DNMNH collection (Appendix 1).The exception to the measurement process described in Goodman *et al*. (2017) was for tip length, which was measured in ventral rather than lateral view, as the curvature of the tip in lateral view was more difficult to measure. Six of the bacula were from individuals that were also sequenced (Appendix 1).

Morphological study

Before specimen preparation five external measurements were taken in millimetres using a ruler from bats caught in the Kruger National Park: forearm length, total length, tail length, ear length, and hind foot length (including the claw). Body mass in grams was recorded with a 10 g Pesola spring balance. Images were also taken of the ear and tragus. Any existing external measurements were also recorded from other specimens that were examined. In instances where a head and body measurement was reported instead of a total length measurement, the total length was calculated adding the head and body measurement to the tail length. The uropatagium of specimens of *A*. cf. *helios* and specimens of *A. nanus* s.l. from the DNMNH collection (Appendix 1) were examined to identify the presence of any glands. Lower molars of specimens of *A*. cf. *helios* and *A. nanus* s.l. from the DNMNH and NHMUK collections (Appendix 1) were observed using a binocular microscope to identify whether they were myotodont or nyctalodont following the descriptions in Happold and Van Cakenberghe (2013) and see Figure 2. Observations of the uropatagium and lower molars for the holotype of *A. helios* were made by Don Wilson (pers. comm., 2011).

Ten cranio-dental measurements were taken: condylo-incisor length (CIL), braincase height posterior to the bullae (BH), braincase breadth (BB), post-orbital width (POW), width of the foramen magnum (WFM), width of the mandibular fossa articular surface (WAS), width across the outer surfaces of upper canines (WOUC), width between inner surfaces of the upper first molars (WIUM1), lateral-medial width of the fourth upper premolar (WUPM4), and anterior-posterior length of the upper first molar (LUM1). These measurements followed those selected by Kearney and Taylor (2011) for analysis of *A. nanus*, but excluded zygomatic width that is often broken, and the length of the mandible between the outside edges of the coronoid and condylar processes, which was not measured on specimens in collections in Europe. Measurements were made by TK from 101 specimens using Mitutoyo digital calipers accurate to 0.1 mm (Appendix 1). Measurements of the holotype of *A. helios* were made by Don Wilson (pers. comm., 2011). Sixteen of these specimens were also sequenced (Appendix 1).

Statistical analyses

The measurements were not transformed or scaled for any of the analyses. Measurements of the skull were used in principal component analyses (PCA) based on covariance matrices. A non-parametric, one-way permutational multivariate analysis of variance (PERMANOVA) based on a Euclidian similarity index, which excluded the holotype of *A. helios*, was also run on the cranio-dental measurements. *Afronycteris helios* was excluded from the PERMANOVA as a PERMDISP test was significant when it was included in the dataset (F 4.49, *P* 0.01), but not significant when it was excluded (F 2.70, *P* 0.072). Differences in skull and external morphology between taxa (excluding the holotype of *A. helios*) were also assessed with one-way Kruskal-Wallis and Dunn's post-hoc pairwise tests. Individuals were assigned *a priori* classifications to different taxa based on name bearing type status, clustering within the PCA plot of the first two principal coordinates of cranio-dental variables, as well as the morphological characteristic of having glands on the uropatagium, and any bacula morphology and sequence information. The statistical analyses were run in PAST 4.17c (Hammer *et al*. 2001), with significance at $P < 0.05$.

Results

Molecular genetics

From the 15 specimens included for molecular genetics (Appendix 1), sequences for the Cytb and 12S regions were obtained for all 15, while only 5 were obtained for the COI region largely due to difficulty with amplification and limited availability of extracted material. Variable numbers of representative sequences were available from the public repositories for the three different regions accounting for the differences in representation of genera between the various analyses. As there was no tissue available for *A. helios* senso stricto, or prior sequences in online sources, it was not represented in these analyses.

A higher number of representative Cytb (Figure 3) sequences were available from literature for inclusion in the molecular analyses than for COI (Figure S1) and 12S (Figure S2), which is likely because it is the most variable gene among the three targeted and most suitable for assessing lineage-level differences. The sequences generated in this study grouped in four different clades with posterior probabilities of 1, 0.78, and 1 respectively. The first was represented by *Afronycteris* **sp. nov.**, while the other three clades represented *A. nanus* from different Sub-Saharan

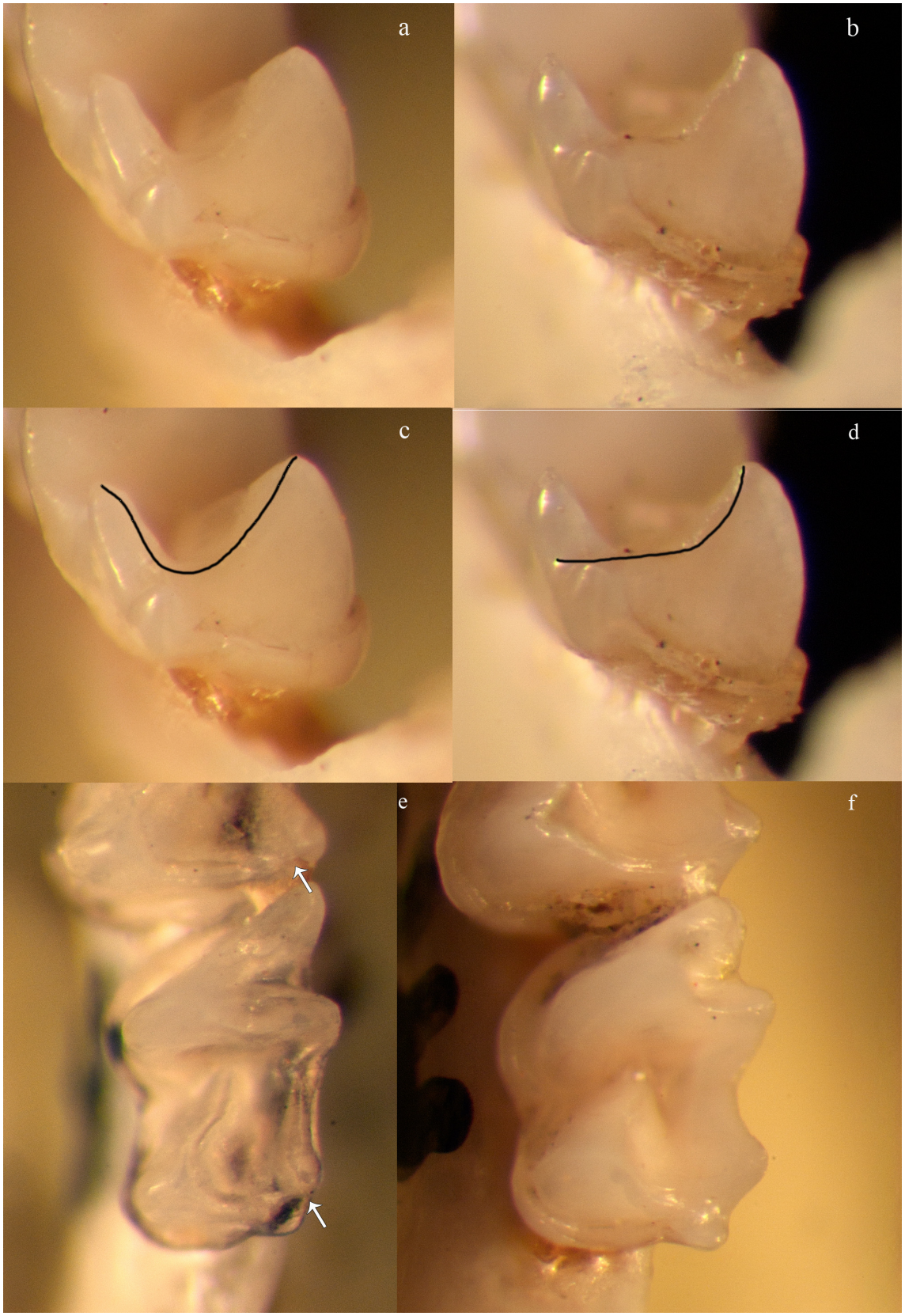

FIGURE 2. Views of lower molar teeth showing the a) myotodont form (TM 46480) and b) nyctalodont form (TM 50951) as seen from the posterior surface of the third molars, with repeat images of these teeth that includes a black line to indicate postcristid ridge (c and d). Views of the occlusal surface of the second and third myotodont molars, indicating e) with white arrows where there is a gap between the postcristid ridge and the entoconid (TM 48573), and f) the postcristid ridge connecting to the entoconid without a gap (TM 46480).

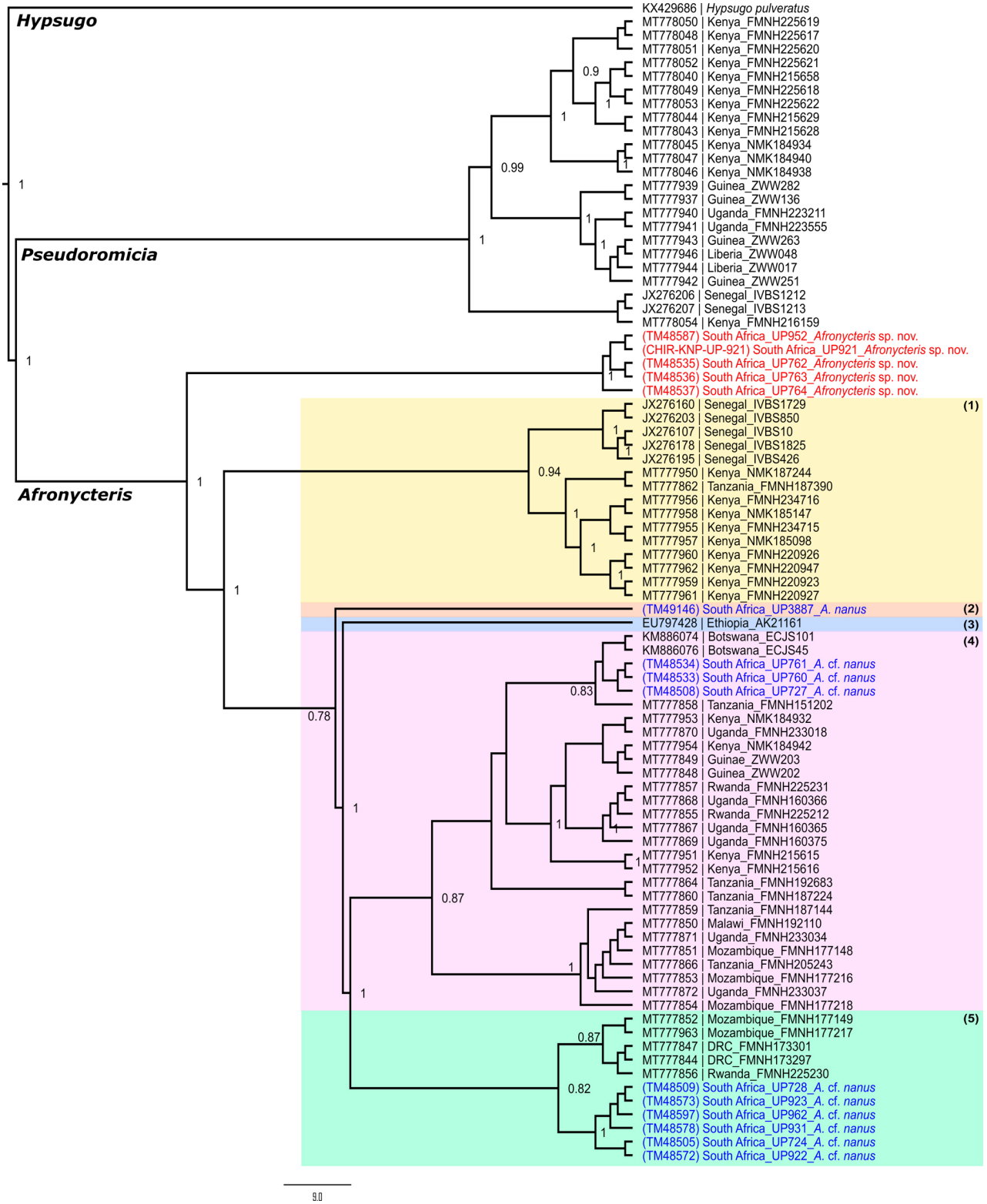

FIGURE 3. Bayesian phylogenetic analysis based on cytochrome oxidase b (Cytb) sequences (938nt) from species in the Vespertilionidae family (TPM2uf+I+G substitution model based on the Bayesian information criterion (BIC)). Genera are indicated at internal branching points. The phylogenetic position of *Afronycteris* **sp. nov.** is indicated in red, other *Afronycteris* sequences generated in this study from specimens collected in the northern part of South Africa are indicated in blue and representative sequences from literature is represented in black. Museum numbers of specimens from which sequences were generated are indicated in brackets. Clades used for p-distance calculations are represented by bracketed numbers and overlaid with different colours. The Bayesian phylogeny was constructed using BEAST v2.6.6. Only posterior probabilities of >0.5 are indicated.

localities. Of the *A. nanus* clades the first was represented by an individual from Ga Mafefe, South Africa (TM 49146), the second included individuals from the Makuleka Contract Park, South Africa (TM 48508, 48533 and 48534) with individuals from Botswana, Guinea, Kenya, Malawi, Mozambique, Rwanda, Tanzania, and Uganda, and the third included the remaining six sequences of individuals from the Makuleka Contract Park, South Africa together with individuals from the Democratic Republic of Congo, Mozambique, and Rwanda.

Sequence differences between individuals for all three genome regions are provided in Tables S1–S3, with ranges and means of Cytb for different groups indicated in Table 1 and Figure 4. *Afronycteris* **sp. nov.** showed sequence divergences of 6.4–10% from the other *A. nanus*. Within *A. nanus*, the clade with individuals from Kenya, Senegal, and Tanzania were most different to the other *A. nanus* (4.4–7.9%). The individual from Ga Mafefe, South Africa (TM 49146) was also considerably different (4.6–4.8%) from all other *A. nanus*. The remaining clades of *A. nanus* that included sequences of South African specimens generated in this study, one with individuals from Botswana, Guinea, Kenya, Malawi, Mozambique, Rwanda, Tanzania, and Uganda, and the other with individuals from the Democratic Republic of Congo, Mozambique, and Rwanda were more similar (0.5–1.7%).

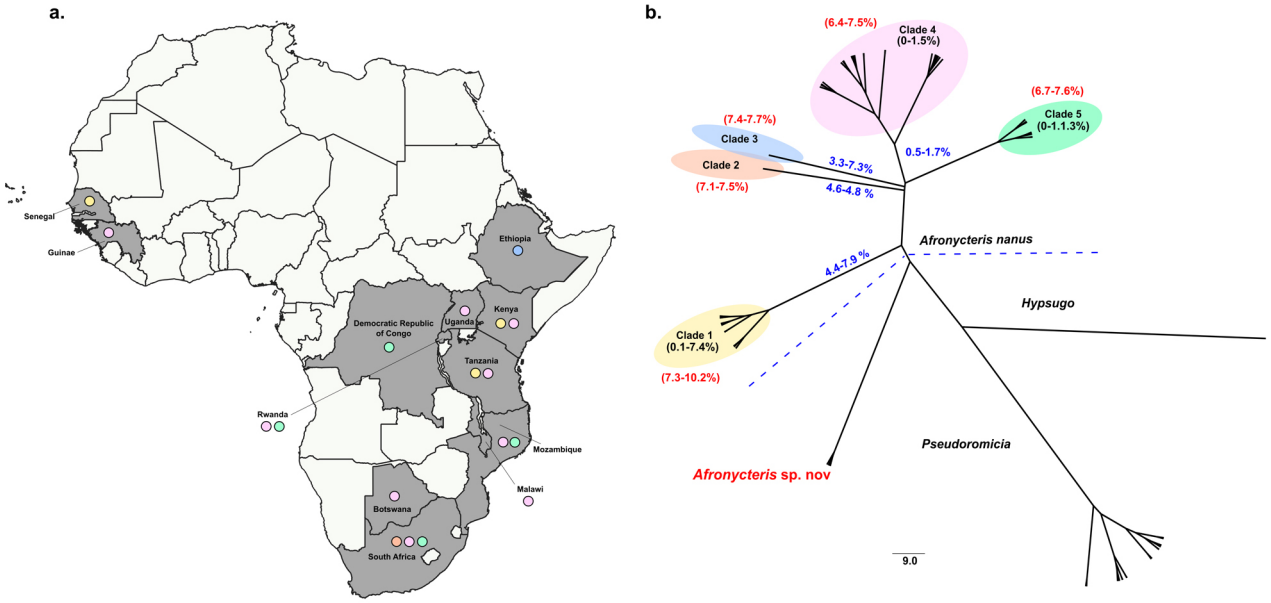

FIGURE 4. Regional cytb sequences of *Afronycteris* represented in the phylogenetic analyses. a) African countries represented with sequence information are represented in dark grey. Clades associated with each region are indicated in colour circles. b) Radial representation of the cytb analyses with percentage differences indicated. Red: clade comparison with *Afronycteris* sp. nov; Black: within clade divergence; Blue: clade divergence with other *A. nanus* clades.

TABLE 1. Mean uncorrected pairwise Cytb distances between *Afronycteris* **sp. nov.** from South Africa and *A. nanus* from 1—Kenya, Senegal and Tanzania, 2—Ga Mafefe, South Africa, 3—Ethiopia, 4—Botswana, Guinea, Kenya, Malawi, Mozambique, Rwanda, South Africa, Tanzania, Uganda, and 5—DRC, Mozambique, Rwanda, South Africa (below the diagonal), and within (in bold along the diagonal).

	A. rautenbachi **sp. nov.**	*A. nanus* (1)	*A. nanus* (2)	*A. nanus* (3)	*A. nanus* (4)	*A. nanus* (5)
Afronycteris **sp. nov.**	**0.002 (0.001–0.005)**					
A. nanus (1)	0.082 (0.073–0.102)	**0.033 (0.001–0.074)**				
A. nanus (2)	0.073 (0.071–0.075)	0.052 (0.044–0.072)	**NA**			
A. nanus (3)	0.075 (0.074–0.077)	0.056 (0.046–0.073)	0.048	**NA**		
A. nanus (4)	0.068 (0.064–0.075)	0.058 (0.045–0.079)	0.048 (0.046–0.051)	0.037 (0.033–0.041)	**0.007 (0–0.015)**	
A. nanus (5)	0.071 (0.067–0.076)	0.058 (0.048–0.079)	0.049 (0.046–0.052)	0.038 (0.036–0.041)	0.011 (0.005–0.017)	**0.007 (0–0.013)**

For the COI analyses (Figure S1), the same observation of three larger clusters was observed as described for the Cytb analysis, although a lower degree of genetic variation was observed within the COI region. Sequence divergences between *Afronycteris* **sp. nov.** and *A. nanus* from this study and representative sequences from specimens sampled in Liberia and Cote d'Ivoire ranged from 3.4 to 4.1% (Table S2).

A more limited number of representative *Afronycteris* sequences were available for inclusion in the 12S analysis. However, similar phylogenetic clustering (Figure S2) was evident as described for the Cytb and COI analyses. The *Afronycteris* **sp. nov.** sequences clustered distinctively from other *Afronycteris* sequences. Sequence divergences between *Afronycteris* **sp. nov.** and *A. nanus* from four different clades ranged from 2.8 to 3.8% (Table S3).

Baculum morphology

Images (Figure 5) and measurements (Table 2) of the bacula indicated four morphologies among the individuals assessed. Unfortunately, as there were no physical bacula available for examination of *A. helios* senso stricto this species was not represented in these analyses. *Afronycteris* **sp. nov.** had a different, more triangular tip morphology relative to the more rounded tip of the individuals previously identified as *A. nanus* (Figure 5a). Among the individuals previously identified as *A. nanus* there were three bacula morphologies, with differences in overall length, greatest width of the shaft midway along its length, and width and length of the bilobed base, which were unrelated to age that had been assessed by tooth wear. Individuals from Eswatini and south-eastern localities in South Africa had longer bacula with a broader shaft and base (Figure 5b). Those with bacula of an intermediate length, with a narrower shaft, and long base of an intermediate width were from Botswana, Zimbabwe and north-eastern South Africa (Figure 5c). While the smallest bacula morphology in relation to the previously described characters, was found in an individual from north-eastern South Africa (Figure 5d). All the *Afronycteris* bacula showed a similar curvature along the length of the bacula into the dorsal plane, which was best seen in the lateral view. Apart from the difference in the tip shape morphology, the bacula of *Afronycteris* **sp. nov.** was like the larger *A. nanus* bacula on overall length, but more like the intermediate *A. nanus* bacula on width of the shaft midway along the length, and most like the smallest *A. nanus* bacula on greatest width of the base.

TABLE 2. Bacula measurements (in millimetres) of *Afronycteris* **sp. nov.**, *A. nanus, A*. cf. *nanus*—clade 4, and *A.* cf. *nanus*—clade 5. See Appendix 1 for details about which individual bacula were assessed. The information presented is: n = the number of specimens measured, and for each character with more than a single measurement, the figures represent the mean, standard deviation, and the minimum and maximum values.

	n	Greatest length	Greatest width tip	Greatest width base	Width of shaft midway along length	Tip length
Afronycteris **sp. nov.**	1	1.58	0.42	0.57	0.16	0.49
A. nanus	12	1.80 ± 0.14 (1.56–2.08)	0.45 ± 0.03 (0.41–0.53)	0.77 ± 0.05 (0.67–0.86)	0.29 ± 0.02 (0.27–0.35)	0.38 ± 0.04 (0.33–0.46)
A. cf. *nanus*—clade 4	5	1.44 ± 0.11 (1.32–1.55)	0.46 ± 0.06 (0.36–0.52)	0.62 ± 0.05 (0.58–0.70)	0.19 ± 0.02 (0.18–0.22)	0.29 ± 0.07 (0.20–0.35)
A. cf. *nanus*—clade 5	1	1.28	0.36	0.53	0.16	0.31

Six of the 19 individuals whose bacula were assessed were also sequenced with Cytb, and the four baculum morphologies aligned with different Cytb clades. TM 48353 with the triangular tip bacula morphology (Figure 5a) was in the *Afronycteris* **sp. nov.** clade (Figures 3 and 4), while the other bacula morphologies were in different clades of individuals previously identified as *A. nanus*: TM 49146 with the longest bacula (Figure 5b) was in clade 2 (Figures 3 and 4), TM 48533 with an intermediate length bacula having a longer base of intermediate width (Figure 5c), as well as TM 48486 and 48488 were in clade 4 (Figures 3 and 4), while TM 48573 with the shortest bacula and narrowest and shortest base (Figure 5d) was in clade 5 (Figures 3 and 4).

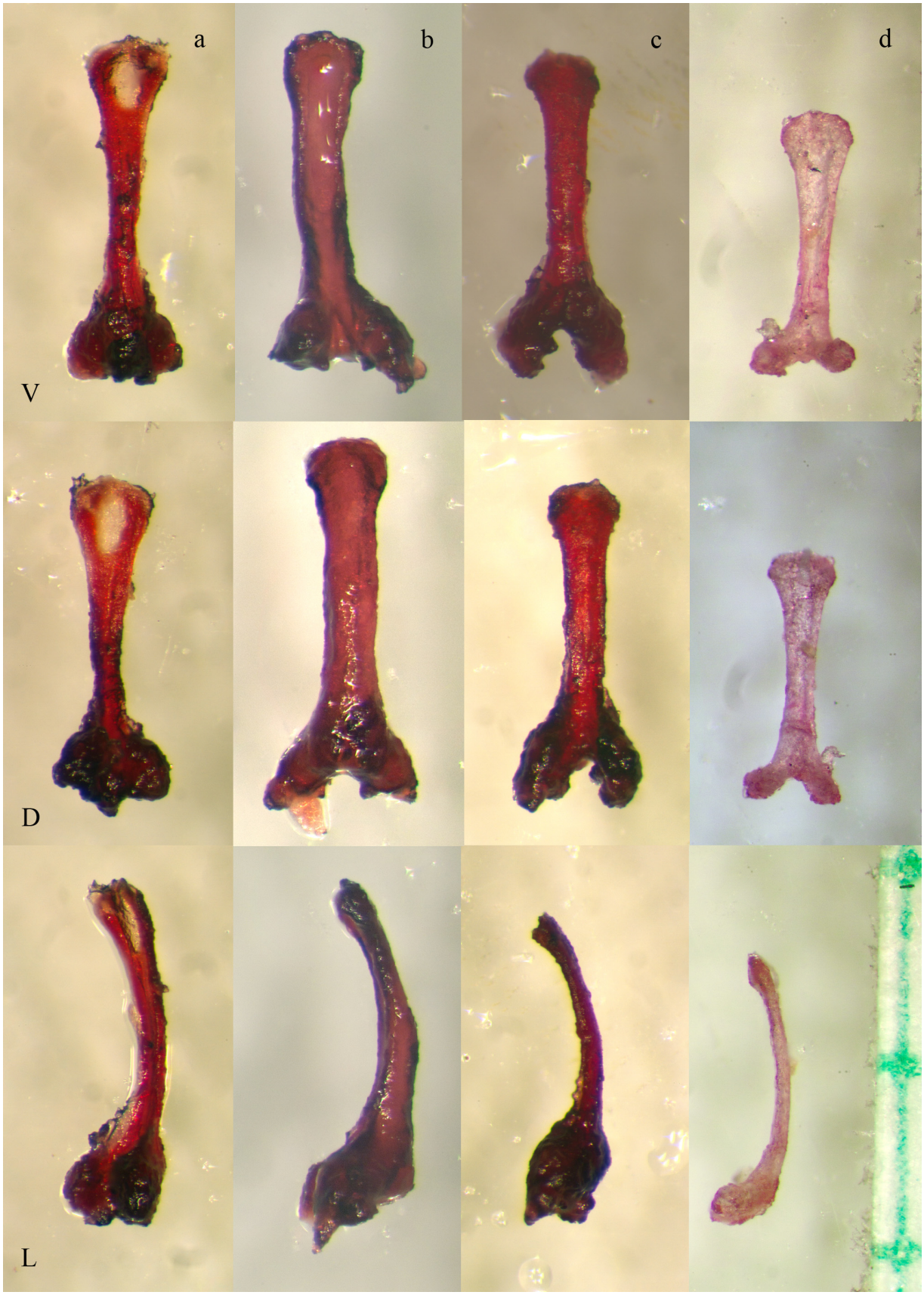

FIGURE 5. Ventral (V), dorsal (D), and lateral (L) views of bacular of a) the holotype, TM 48535, of *Afronycteris* **sp. nov.** from South Africa, Limpopo province, Kruger National Park, Makuleka Contract Park; b) DNSM 5871, *A. nanus* clade 2 from South Africa, KwaZulu-Natal province; c) TM 48533, *A.* cf. *nanus* clade 4 from South Africa, Limpopo province; and d) TM 48573, of *A.* cf. *nanus* clade 5 from South Africa, Limpopo province. The scale in the bottom right image is of 1 mm gradations.

Cranio-dental morphology

The first two coordinates of the PCA of skull measurements contributed 65.54% and 12.00% respectively to the variation. The plot of these principal coordinates showed individuals previously identified as *A. nanus* (including holotypes and syntypes of several synonyms), *A. helios* (the holotype), *A.* cf. *helios* and *Afronycteris* **sp. nov.** (Figure 6) separated diagonally across both coordinates, from the positive second to positive first coordinates. The first coordinate was size related with all measurements having positive loadings, and condyle-incisor length and length of the upper first molar tooth having the highest and least loadings respectively (Table 3). The second coordinate related to braincase shape change with the largest positive loading being braincase height, and the most negative loading being braincase breadth (Table 3).

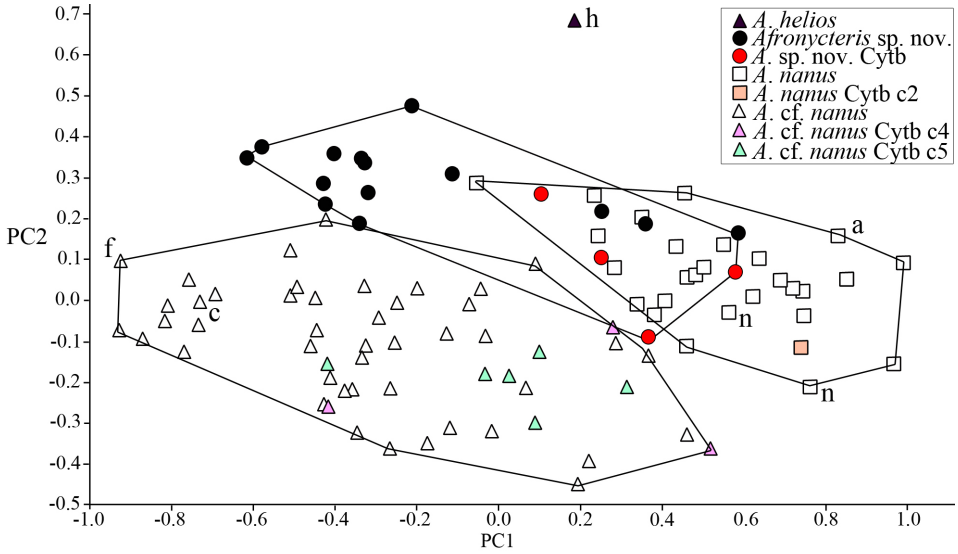

FIGURE 6. Plot of first two principal components based on variance-covariance coefficients of 10 skull measurements from 102 specimens of *Afronycteris* **sp. nov.**, *A. helios*, *A. nanus* and *A.* cf. *nanus* as noted in the FIGURE legend. Symbols of individuals that were sequenced with Cytb are the same colour as clades identified in FIGURES 3 and 4. Holotypes are identified as follows: a = *Pipistrellus nanus australis* Roberts 1913 (TM 1076), c = *Pipistrellus culex* Thomas, 1911 (NHMUK 1911.3.24.4), f = *Pipistrellus fouriei* Thomas, 1926 (NHMUK 1925.12.4.20), and h = *Pipistrellus helios* Heller, 1912 (USNM 181813). Syntypes of *Vespertilio nanus* Peters, 1852 (ZMB 588a and ZMB 588c) are identified by a 'n'.

TABLE 3. Eigenvector loadings from the principal component analysis based on craniodental measurements of *Afronycteris* **sp. nov.**, *A. nanus,* and *A.* cf. *nanus*. Characters weighted highest and lowest on each axis are indicated in bold font.

Character	PC 1	PC 2
CIL	**0.812**	-0.170
BH	0.321	**0.770**
BB	0.212	**-0.454**
POW	0.136	-0.217
WFM	0.179	-0.253
WAS	0.069	0.037
WOUC	0.303	0.205
WIUM1	0.200	-0.061
WUPM4	0.078	0.095
LUM1	**0.024**	0.070
Cumulative explained variation	65.54%	12.00%

The holotype of *A. helios* occupied the morpho-space indicating the largest braincase height and smallest braincase width, whereas most of the individuals identified as *A. nanus* had the inverse with larger braincase breadths and smaller braincase heights, and most of the individuals identified as *A.* cf. *helios* occurred between these extremes. Individuals previously identified as *A.* cf. *helios* from the Democratic Republic of Congo, Kenya, Mozambique, and *Afronycteris* **sp. nov.** from north-eastern localities in South Africa, showed a range of condyle-incisor lengths, with larger individuals being primarily from South Africa, but also included some from Kenya and Mozambique. Larger individuals identified as *A.* cf. *helios* overlapped with smaller individuals in a group that were previously identified as *A. nanus*. Even though there was some overlap between individuals previously identified as *A.* cf. *helios* and *A. nanus*, they did separate at the extremes with *A.* cf. *helios* having slightly larger braincase heights and smaller first upper molar tooth lengths, whereas the *A. nanus* in this group mostly had larger condyle-incisor lengths and wider braincase breaths. The *A. nanus* in this group were from Zimbabwe, Mozambique, Eswatini and South Africa (eastern localities). Included in the group were specimens of two *A. nanus* synonyms, the holotype of *Pipistrellus nanus australis* (Roberts, 1913) (TM 1076) from South Africa, and two syntypes of *Vespertilio nanus* (Peters, 1852) (ZMB 588-1 and ZMB 588-3) from Mozambique. TM 1076 plotted in the morpho-space having one of the longest condyle-incisor lengths and intermediate braincase height and breadths relative to the other specimens in the plot. ZMB 588-1 and ZMB 588-3 plotted relatively close to one another, in the morpho-space relative to TM 1076, having a shorter (ZMB 588-1) and similar (ZMB 588-3) condyle-incisor length, smaller braincase heights, and larger braincase breadths. Six individuals in this group had dissected bacula, all of which were the longer length morpho-type. These *A. nanus* with larger skulls and longer bacula separated along the diagonal of the first and second principal coordinates from other group of individuals also previously identified as *A. nanus*.

The second group of individuals previously identified as *A. nanus* occupied the morpho-space having smaller condyle-incisor lengths, larger braincase breadths and smaller first upper molar lengths relative to the other specimens in the plot. Individuals in this group were from Senegal, The Gambia, Liberia, Nigeria, Republic of Congo, Zambia, Malawi, Namibia, Botswana, Zimbabwe, and South Africa (north-eastern localities). They showed a range of condyle-incisor length, suggestive of size changes in relation to latitude. Individuals from more southerly localities mostly had larger condyle-incisor lengths and first upper molar tooth lengths, while individuals from more northerly latitudes had smaller condyle-incisor lengths and first upper molar tooth lengths. However, there were exceptions, as individuals from Botswana and Namibia occupied the morpho-space with individuals from more northerly localities. This group also included holotype specimens of two *A. nanus* synonyms, *Pipistrellus fouriei* (Thomas, 1926) (BMNH 25.12.4.20) from Namibia, and *Pipistrellus culex* (Thomas, 1911) (BMNH 1911.3.24.4) from Nigeria. Both these type specimens plotted in the morpho-space of smaller condyle-incisor lengths, larger braincase breadths and smaller first upper molar lengths relative to the other specimens in the plot. Five individuals in this group had dissected bacula, all of which were the shorter length morpho-type. Given the individuals with larger bacula and cranio-dental morphology included syntypes of *Vespertilio nanus* (Peters, 1852) these individuals with smaller bacula and cranio-dental characters will be referred to as *A.* cf. *nanus* to distinguish them from the larger morph individuals.

With the exception of *A. helios*, which was excluded as it introduced unequal dispersion in the dataset, the other grouping patterns in the PCA described above, were also identified by the significant PERMANOVA (F 32.57, *P* 0.0001), and Dunn's post-hoc pairwise tests that were significantly different between all the taxa (*A.* **sp. nov.**, *A. nanus,* and *A.* cf. *nanus*).

Four NHMUK specimens previously identified as *A. helios* that had varying degrees of damage to the skulls, which had excluded them from the PCA based on 10 craniodental measurements were assessed in three different PCAs of reduced numbers of variables to exclude variables with missing measurements. Excluding BH and BB for BMNH 1911.12.1.3 and BH, BB, and WFM for BMNH 1912.7.1.28 removed some of the clustering seen in the PCA with 10 characters and the identification of these specimens could not be confirmed with these measurements. Whereas, the PCA having removed WOUC and WIUM1 still resolved taxa clusters as seen with 10 characters (Figure 6) and confirmed that BMNH 1912.7.1.26 and 1912.7.1.32 both clustered with specimens assigned to the new species (Figure S3).

Fourteen individuals included in the PCA analysis were also sequenced with Cytb. Two of the 4 clades resolved by Cytb (Figures 3 and 4) were also differentiated in the PCA of cranio-dental measurements (Figure 6). These were the clade distinct from other *A. nanus—Afronycteris* **sp. nov.**, and clade 2 of specimens previously identified as *A. nanus*, which were cranio-dentally larger than other individuals previously identified as *A. nanus*. While baculum

morphology was able to differentiate between smaller individuals of *A*. cf. *nanus* (Figure 5) from clades 4 and 5 in the Cytb phylogeny (Figures 3 and 4), they were not separated by the cranio-dental measurements (Table 4) used in the PCA (Figure 6).

TABLE 4. Craniodental measurements (in millimetres) of *Afronycteris* **sp. nov.**, the holotype of *A. helios*, *A. nanus,* and *A.* cf. *nanus*. The information presented is the mean, the standard deviation, and the minimum and maximum values. The last row contains the Kruskal-Wallis H-value and probability results for tests between taxa with more than one individual. The craniodental measurement abbreviations are explained in the materials and methods section.

	n	CIL	BH	BB	POW	WFM
A. helios	1	11.1	4.96	5.8	3.36	2.83
Afronycteris **sp. nov.** Holotype TM 48535	1	11.01	4.57	5.85	3.33	3.23
Afronycteris **sp. nov.** (other specimens)	17	10.80 ± 0.36 (10.40–11.42)	4.44 ± 0.12 (4.26–4.69)	5.93 ± 0.18 (5.60–6.25)	3.29 ± 0.13 (3.07–3.54)	3.05 ± 0.07 (2.95–3.20)
A. nanus	29	11.36 ± 0.22 (10.85–11.77)	4.49 ± 0.10 (4.26–4.69)	6.08 ± 0.14 (5.79–6.39)	3.44 ± 0.11 (3.18–3.66)	3.23 ± 0.13 (2.97–3.46)
A. cf. *nanus*	54	10.75 ± 0.32 (10.20–11.34)	4.10 ± 0.15 (3.82–4.43)	6.03 ± 0.18 (5.62–6.38)	3.38 ± 0.12 (3.04–3.65)	3.10 ± 0.15 (2.86–3.46)
ANOVA		39.62, $P > 0.000$	96.4, $P > 0.000$	5.17, $P = 0.007$	7.91, $P > 0.000$	12.25, $P > 0.000$

.....continued below

TABLE 4. (Continued)

	n	WAS	WOUC	WIUM1	WUPM4	LUM1
A. helios	1	1.48	3.35	2	0.9	0.84
Afronycteris **sp. nov.** Holotype TM 48535	1	1.27	3.38	2.22	0.85	0.93
Afronycteris **sp. nov.** (other specimens)	17	1.16 ±0.10 (0.93–1.32)	3.49 ±0.11 (3.32–3.71)	2.21 ± 0.09 (2.01–2.33)	0.92 ±0.04 (0.87–1.04)	0.97 ± 0.05 (0.91–1.09)
A. nanus	29	1.16 ± 0.12 (0.97–1.37)	3.67 ± 0.09 (3.46–3.81)	2.40 ± 0.09 (2.19–2.59)	0.85 ± 0.12 (0.64–1.04)	0.97 ± 0.08 (0.82–1.09)
A. cf. *nanus*	54	1.14 ± 0.10 (0.89–1.40)	3.34 ± 0.12 (3.13–3.69)	2.22 ± 0.10 (1.98–2.44)	0.79 ± 0.06 (0.63–0.96)	0.92 ± 0.06 (0.78–1.06)
ANOVA		0.95, $P = 0.3912$	79.53, $P > 0.000$	38.57, $P > 0.000$	19.08, $P > 0.000$	6.46, $P = 0.002$

Lower molar character

A magnification of x35 and oblique lighting was found to assist in the identification of this morphology. Of the 39 specimens of *Afronycteris* examined (Appendix 1) 33 were assessed as having entirely myotodont lower molar morphology (as shown in Figure 2). The direction of the postcristid ridge toward the entoconid was particularly clear when observed with the teeth at an angle and using an oblique light source to illuminate the posterior surface of the postcristid ridge. Exceptions to the myotodont morphology were observed in six specimens that had a combination of both morphologies on different lower molar teeth. In each case one of the three lower molars had a more nyctalodont morphology while the other two were myotodont. In TM 34223, 34607, 48508 (*A*. cf. *nanus*) and TM 34609 (*A*. *nanus*) the nyctalodont tooth was the first molar, whereas in TM 48535 and 50951 (*Afronycteris* **sp. nov.**) it was the third lower molar that was more nyctalodont. In teeth that were worn the path of the postcristid ridge heading in the direction of the entoconid cusp was less obvious. Considerable wear on the teeth made the myotodont morphology more difficult to identify and might on cursory observation be mistaken for the nyctalodont form.

An alternative to the myotodont morphology described by Happold and Van Cakenberghe (2013) and illustrated in their Figure 138, page 604, was also observed. As with their myotodont description, the path of the postcristid ridge went from the hypoconulid toward the entoconid, but did not connect to the entoconid, instead it ended at the base of the entoconid (Figure 2). This morphology was not considered to be the nyctalodont form described by Happold and Van Cakenberghe (2013) where the postcristid ridge runs into the gap between the hypoconulid and the side of the molar. In specimens with less tooth wear (*A*. cf. *nanus*—TM 34607, 48488, and *A*. *nanus* TM 35284 and

35285) this was seen by a clearly defined groove at the end of the postcristid ridge and the base of the entoconid, with the groove extending to also separate out the hypoconulid. In a specimen of *A*. cf. *nanus* with more tooth wear (TM 48573) the lack of connection between the postcristid ridge and the entoconid could also be seen in the worn down 'scar' of the ridge that ended with an unworn region at the base of the entoconid, which correlated with the 'groove' region observed in specimens with less tooth wear.

External morphology

External measurements (Table 5), albeit with some exceptions, also roughly separated individuals into the same groups as indicated in the PCA based on cranio-dental measurements. Generally, the external measurements of *A. nanus* were largest and those of *A*. cf. *nanus* smallest, with the measurements of *A. helios* and *Afronycteris* **sp. nov.** being intermediate. The holotype of *A. helios* had a larger total length and smaller tail, ear, forearm lengths and mass than most specimens of the new species, while their hindfoot measurements were similar. An exception, such as SMF 92761 (*A*. cf. *nanus*), which was one of the smallest skulls in the PCA based on skull measurements (Figure 6) and yet had much larger external measurements than other individuals in the *A*. cf. *nanus* group, might be accounted for by inconsistencies in measurements being made by many different people at different points in time. Exceptions in relation to mass were in most instances associated with individuals weighing more because of being pregnant or scrotal.

TABLE 5. External measurements (in millimetres) and mass (in grams) of the holotype of *A. helios*, *Afronycteris* **sp. nov.**, *A. nanus* and *A.* cf. *nanus*. The information presented is the mean, the standard deviation, and in parentheses the minimum and maximum values and the number of specimens. The last row contains the Kruskal-Wallis H-value and probability results for tests between taxa with more than one individual. HF = hind foot length, FA = forearm length.

	Total	Tail	Ear	HF (cu)	FA	Mass
A. helios	76	31	9	5	27.5	none
Afronycteris **sp. nov.** Holotype TM 48535	73	31	10	6	30	3.8
Afronycteris **sp. nov.** (other specimens)	72.6 ± 3.72 (66.0–78.0, n = 10)	32.1 ± 1.67 (29.5–35.0, n = 10)	9.5 ± 1.34 (8.0–11.0, n = 10)	5.1 ± 0.98 (4.0–6.5, n = 10)	31.3 ± 0.33 (30.9–31.7, n = 6)	4.2 ± 0.62 (3.7–5.3, n = 6)
A. nanus	74.3 ± 3.45 (68.0–78.0, n = 12)	33.9 ± 2.71 (29.0–37.0, n = 12)	10.5 ± 1.03 (8.0–12.0, n = 12)	5.8 ± 1.03 (4.0–7.0, n = 12)	30.8 ± 2.28 (29.4–37.5, n = 12)	3.4 ± 0.32 (2.8–3.9, n = 12)
A. cf. *nanus*	68.9 ± 6.11 (56.8–92.4, n = 35)	30.0 ± 3.29 (20.0–39.2, n = 35)	9.7 ± 0.95 (7.2–11.5, n = 35)	5.7 ± 1.04 (4.2–10.5, n= 35)	28.8 ± 1.32 (26.1–33.1, n = 35)	3.4 ± 0.58 (2.4–4.5, n = 22)
ANOVA	5.65, $P = 0.006$	8.55, $P = 0.001$	3.02, $P = 0.057$	1.47, $P = 0.24$	11.16, $P > 0.000$	6.67, $P = 0.003$

The presence or absence of glands on the uropatagium was assessed in 56 of the specimens included in the previous analyses (Appendix 1). Of the 17 that were genotyped, a pair of glands on the uropatagium, with one on either side of the tail (Figure 7) was present in all five of the *Afronycteris* **sp. nov.** specimens, but not in any of the *A. nanus* (n=1), *A*. cf. *nanus* clade 4 (n=5) or *A*. cf *nanus* clade 5 (n=6) specimens (Figures 3 and 4). Among the non-genotyped specimens, no glands were found on the uropatagium of specimens previously identified as *A. nanus*. The uropatagium of the holotype of *A. helios* also had no glands (pers. comm., 2011). However, of the non-genotyped specimens previously identified as *A. helios* 12 had a pair of glands on the uropatagium, five had only one gland (three being on the left side and two on the right side of the tail), and one had none. Besides lacking glands on the uropatagium BMNH 75.2556 was also missing inner upper incisors and had probably been misidentified as *A. helios*.

FIGURE 7. Uropatagium of *Afronycteris* **sp. nov.** showing the glands on either side of the tail bones, viewed ventrally in CHIR-KNP-UP-921 (left), and dorsally in TM 48587 (right).

Where glands were present, they could be observed on the uropatagium of both wet and dry study skins. The gland colour was usually similar too, but darker than, the uropatagium membrane colour. In a few specimens the glands were yellowish in colour (e.g. BMNH 1912.7.1.30 and 1912.7.1.32), but in others they were paler and more indistinct (e.g. BMNH 1912.7.1.27). In most individuals the glands were of a consistent colour, although in TM 48535 much of the outer edges were darker than the rest of the gland. The opacity of the glands also varied with some being more translucent, albeit not to the same degree as the uropatagium membrane (e.g. TM51005), while others were opaquer (e.g. TM 50951). The glands where almost circular to oval in shape and varied slightly in shape and size between individuals and between a pair. Diameter measurements of glands on DNMNH specimens indicated a range in size from 1.5 x 1.0 mm to 3.0 x 2.5 mm.

Conclusions based on molecular genetics, skull, baculum and external morphology

Unfortunately, *A. helios* sensu stricto is so poorly known (Monadjem *et al*. 2021) as to have only been included in these analyses by cranio-dental morphology of the holotype and details from the initial description. Nevertheless, the genetic and various morphological results provided above for Vespertilionidae bats from Africa showed the distinction of individuals previously referred to as *A*. cf. *helios*, which we herein formally describe.

Systematics

Family Vespertilionidae Gray, 1821

Genus *Afronycteris*

Afronycteris rautenbachi sp. nov.

urn:lsid:zoobank.org:act:AFE05864-DE86-4019-8D02-010E320C7936

Synonymy

Pipistrellus nanus O'Shea, 1980; Happold and Happold, 1996, in part.
Pipistrellus (*Hypsugo*) *helios* Hill and Harrison, 1987, in part.
Pipistrellus cf. *helios* Happold and Van Cakenberghe, 2013.
Neoromicia cf. *helios* Geldenhys *et al*., 2018.
Neoromicia helios Harima *et al*., 2023.

Holotype. Ditsong National Museum of Natural History (TM) 48535, adult male prepared as a fluid specimen with skull removed and cleaned, and baculum removed and cleaned. Field number UP-762. The holotype was used in the molecular, morphological and bacula results presented here.

Type locality. South Africa: Limpopo province, Kruger National Park, Makuleka Contract Park, in a Lala palm grove on the edge of a dry pan, -22.34657 S 31.11595 E (Figure 1). Mist-netted on 3 February 2010.

Referred specimens (based on sequence and other morphological characteristics): TM—48536, 48537, 48587, and CHIR-KNP-UP-921 (Appendix 1 for specimen details, Figure 1).

Referred specimens (based on morphological characteristics): BMNH—1911.12.1.4, 1912.7.1.22, 1912.7.1.24, 1912.7.1.27, 1912.7.1.28, 1912.7.1.29, 1912.7.1.30, 1912.7.1.31, 1969.207, 1975.2556, HZM—1.4085, 3.4087, 4.4088, and TM 50951 (see Appendix 1 for specimen details, Figure 1).

Etymology. This species is named in honour of Igantius ("Naas") L. Rautenbach (1942–2024) who was head of the mammal section at Ditsong National Museum of Natural History (formerly Transvaal Museum) from 1968 to 1991, and then the director of the museum from 1991 to 1999. He conducted extensive field research on southern African mammals, including the northern part of the Kruger National Park, which considerably increased the size of the museum collection. Over the years he managed various research collaborations that started with field collection and resulted in numerous publications. The proposed English common name is Kruger tail-gland bat.

Diagnosis. *Afronycteris rautenbachi* is a small Vespertilionidae and among the smallest of the Vespertilionini, being most similar in size and appearance to *A. nanus, A.* cf. *nanus* and *A*. *helios*. *Afronycteris rautenbachi* has a pair of glands on the uropatagium on either side of the tail, near the body (Figure 7).

Description and comparisons. *External characters*. In general, the description by Happold and Van Cakenberghe (2013) of *A*. cf. *helios* was similar to that for specimens assigned here to *A. rautenbachi*. The dorsal pelage in *A. rautenbachi* is long and varied in colour between individuals being pale brown to golden brown. Individual hairs are dark blackish brown colour at the base, with the ends being pale brown or golden brown. The description by Happold and Van Cakenberghe (2013) of the dorsal hairs of *A*. cf. *helios* being tricoloured was not observed. The ventral pelage in *A. rautenbachi* also varies between individuals being pale brown to creamy brown. Individual hairs are dark blackish brown at the base, with ends being pale brown or creamy brown. The wing membranes are a medium brown to dark brown colour, with the uropatagium being slightly paler and more translucent than the wings. The calcars are a translucent white colour. This colour extends from the calcar toward the tail in a narrow band on the edge of the uropotagium membrane for about two thirds of the way, then changes back to the translucent brown colour of the uropatagium for the last section before it meets the tail. The ears and tragus are a slightly lighter coloured brown than the wing membranes. The naked skin on the muzzle and chin is a similar medium brown to dark brown colour as the wing membrane, being paler and slightly pinker around the eyes and mouth (Figure 8). Ears are naked with a rounded tip. The tragi was not measured; however, images indicated their length is less than half the ear length (Figure 9). In contrast to the tragus shape of *A*. cf. *helios* indicated by Happold and Van Cakenberghe (2013) being like that of *P. tenuipinnis* in their illustration Figure 136c (page 601) the shape is more like their illustration of *A. nanus* (Figure 136b, page 601). The tragi broaden toward the tip extending further out on the anterior side, giving a slanted broad distal edge that also projects more anteriorly (Figure 9). Comparing *A. rautenbachi* and sympatric *A*. cf. *nanus* from the Makuleka Contact Park in the north-eastern part of South Africa, the ears of *A. rautenbachi* appear narrower at the widest part, with a less pronounced posterior extension and curvature of the outer, posterior margin of the ear (Figure 9). In the same comparison, while the tragi of both *A*. cf. *nanus* and *A. rautenbachi* have a similar hatchet shape, those of *A. rautenbachi* are broader at the tip, with a more pronounced anterior extension at the tip than in *A*. cf. *nanus* (Figure 9)

What is assumed to be a pair of glands can be observed on either side of, and close to, the tail bones (Figure 7). These are just beyond the level of the fur that extends onto the uropatagium. In the holotype their shape is round and oval (left 1.5 x 1.5 mm, right 1.0 x 1.5 mm), being slightly darker than the tail membrane, but still with a somewhat translucent appearance. Van Cakenberghe and Happold (2013) reported a slightly larger maximum dimension of 3.8 mm than recorded here. These glands were not recorded in *A*. *nanus* and *A*. cf. *nanus*.

Even though there is overlap in the ranges of the external measurements between taxa, Kruskal-Wallis tests between *A. rautenbachi*, *A. nanus* and *A*. cf. *nanus* are significantly different for total, tail and forearm lengths and mass, but not ear and hind foot length (Table 5). As differences in mass could have been biased by pregnant and scrotal individuals this was not considered useful, and Dunn's post-hoc pairwise comparisons were only run to identify significant differences between the taxa for total, tail and forearm lengths. Total and tail lengths of *A. rautenbachi* and *A. nanus* are significantly larger than *A*. cf. *nanus*, and forearm lengths of *A. rautenbachi* and *A. nanus* are significantly larger than *A*. cf. *nanus*, but there is no external measurement differentiating *A. rautenbachi* from *A. nanus*. In comparison with the holotype of *A. helios* the mean external measurements of *A. rautenbachi* are

usually slightly larger, although forearm length is considerably larger than *A. helios* (Table 5). Only total length is longer in *A. helios* than *A. rautenbachi*.

The forearm measurements reported for *A*. cf. *helios* by Van Cakenberghe and Happold (2013), with a mean of 28.0 mm, and a range of 26–30 mm, were smaller than recorded here for *A*. *rautenbachi*, with their largest measurement being the same as the smallest measurement reported here (Table 5). Given there appeared to be cranio-dental size variation associated with longitudinal distribution, as larger individuals were usually from more southerly localities, this might be the result of geographic variation and having had fewer samples from more southerly localities.

FIGURE 8. Lateral head and shoulder view of *Afronycteris rautenbachi* in the hand, of the holotype TM 48535 (left), and TM 48537 (right), both from South Africa, Limpopo province, Kruger National Park, Makuleka Contract Park.

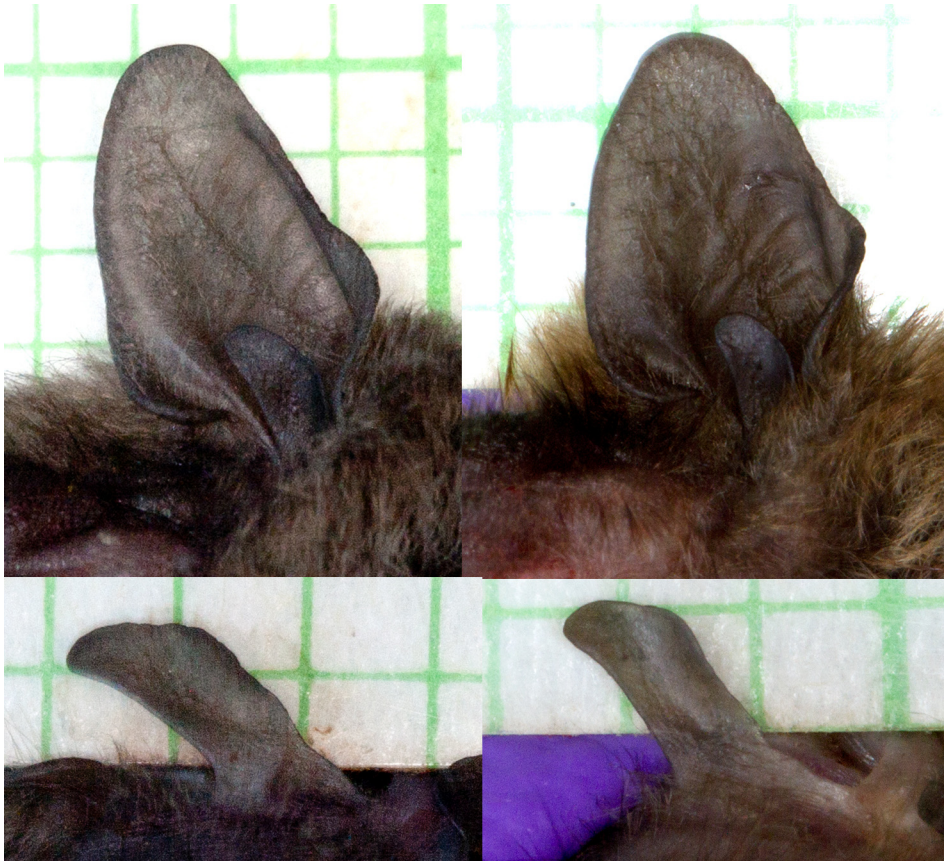

FIGURE 9. Images of ears (above) and tragi (below) of *Afronycteris rautenbachi*, TM 48537 (left) and *A.* cf. *nanus* TM 48572 (right), both from South Africa, Limpopo province, Kruger National Park, Makuleka Contract Park.

Cranio-dental characters. Even though all the cranio-dental variable ranges within taxa overlapped those of other taxa (Table 4), the PERMANOVA is significantly different (F 32.57, *P* 0.0001). In the pairwise comparisons *A. rautenbachi*, *A. nanus* and *A.* cf. *nanus* are all significantly different. The mean cranial measurements of *A. rautenbachi* when compared with the holotype of *A. helios* are only larger for braincase breadth and width of the foramen magnum. All four dental measurements are all slightly larger in the mean for *A. rautenbachi* than the holotype of *A. helios*. Kruskal-Wallis tests between *A. rautenbachi*, *A. nanus* and *A.* cf. *nanus* for each variable are also significantly different for most measurements (Table 4), the exception being the width of the articular surface. Dunn's post-hoc pairwise comparisons indicate how *A. rautenbachi* differs significantly in the width between the canines being narrower than in *A. nanus*, but larger than *A. cf. nanus*, the post-orbital width is smaller than *A. nanus* and *A. cf. nanus*, and the width of the fourth upper premolar in *A. rautenbachi* is wider than in either *A. nanus* or *A. cf. nanus.* The post-hoc comparisons also indicated how *Afronycteris rautenbachi* is significantly different from *A. nanus* in having a smaller braincase breadth, condyle-incisor length, width of the foramen magnum and width between the upper first molar teeth. And, *Afronycteris rautenbachi* **sp. nov.** also differs significantly from *A. cf nanus* in having a taller braincase and longer first upper molar length.

As previously reported for *A. nanus* and *A.* cf. *helios* (Van Cakenberghe and Happold, 2013), the cranium region of *A. rautenbachi* also rises quite sharply from the rostrum (Figure 10), but in lateral view it is observed that the deflection point resulting in the concave profile is further forward in *A. rautenbachi* and *A.* cf. *nanus* than in *A. nanus*. This, together with the overall shape of the cranium being more rounded and expanded in *A. rautenbachi* and *A.* cf. *nanus* than in *A. nanus*, gives the appearance of the lateral rostrum profile being slightly less concave with a shorter rostrum than in *A. nanus*. The interparietal length of *A. rautenbachi* is longer than *A.* cf. *nanus* and more similar to *A. nanus*. As in *A. nanus* and *A.* cf. *nanus* the lambdoid crest in *A. rautenbachi* is more pronounced in older individuals. The zygomatic arches of *A. rautenbachi* are narrow and of a similar width along their length, and slightly broader than *A.* cf. *nanus* and narrower than *A. nanus*. Unlike *A. rautenbachi* and *A.* cf. *nanus* the posterior region of the zygomatic arch in *A. nanus* broadens into the ventral plane.

The dental formula for *A. rautenbachi* is the same as *A. nanus* and *A.* cf. *nanus*; being I2/3, C1/1, PM2/2, M3/3. As in *A. nanus* and *A.* cf. *nanus* the outer upper incisor in *A. rautenbachi* is almost the same height as the first. The inner upper incisors are slightly bifid, with the inner cusp being taller than the outer one, which is no longer visible with increasing wear on the tooth tip. The bifid cusps are positioned with the outer one being sightly posterior to the inner one, following the curvature of the toothrow and being positioned next to the cusp of the outer incisor. The outer cusp of the inner upper incisor and cusp of the outer incisor are a similar height. Relative to *A. nanus* the upper and lower canines of *A. rautenbachi* and *A.* cf. *nanus* have a smaller basal area. The minute upper premolars of *A. rautenbachi* and *A.* cf. *nanus* appear similar in size and slightly smaller than in *A. nanus*, and are found on the lingual side between the canine and next premolar. In *A. rautenbachi* and *A.* cf. *nanus* the cusp patterns of the other upper and lower premolar and molar teeth are similar to *A. nanus*. The anterior end of the dentary bone at the symphysis appears to be broader in *A. nanus* that *A. rautenbachi* and *A.* cf. *nanus.*

Baculum characters. Measurements of the baculum of the holotype of *A. rautenbachi* are given in Table 2. As indicated in Figure 5 the baculum of the holotype of *A. rautenbachi* is similar to the baculum of BMNH 1939.133 from Kenya illustrated in Figure 6d (page 289) by Hill and Harrison (1987) and copied in Happold and Van Cakenberghe (2013) in their illustration Figure 141d (page 605). Hill and Harrison (1987) identified this individual, as well as BMNH 1969.207 and HZM 2.4086, whose bacula were also examined, as *P. helios*. All these individuals had glands on the uropotagium, as a result of which Happold and Van Cakenberghe (2013) referred to BMNH 1939.133 as *P.* cf. *helios*. The skull is still in the specimen of BMNH 1939.133 and that of HZM 2.4086 was broken, but BMNH 1969.207 was measured and here referred to *A. rautenbachi*. The baculum of the holotype of *A. rautenbachi* does not have a distinct tip region, given it widens evenly in line with the shaft, which narrows toward the base. In comparison with *A. nanus* and *A.* cf. *nanus* the tip is more triangular and less rounded in shape, although the top edge of the tip is slightly convex in shape. In BMNH 1939.133 the top edge of the tip is flatter, which may be due to geographic variation. As with the baculum of BMNH 1939.133 (viewed by TK in 2011), the base of the holotype of *A. rautenbachi* (TM 48535) is not entirely cleared of surrounding tissue, which somewhat obscures the details of the base. Nevertheless, the base appears to be short with two lobes, being shorter and narrower than *A. nanus* and *A.* cf. *nanus* clade 4, but longer and broader than *A.* cf. *nanus* clade 5. In lateral view the baculum curves slightly from tip to base with the basal lobes extending into the ventral plane, in a manner similar to *A. nanus* and all *A.* cf. *nanus*.

FIGURE 10. Dorsal ventral and lateral views of the cranium and a lateral view of the mandible of the holotype, TM 48535, of *Afronycteris rautenbachi* from South Africa, Limpopo province, Kruger National Park, Makuleka Contract Park. All images were scaled to the same size. Scale bar = 3 mm.

Distribution and natural history. The full extent of the distribution of *A. rautenbachi* and its natural history are currently unknown given the previous confusion of this species with *A. helios* (Hill and Harrison, 1987) and *A. nanus* (O'Shea, 1980), and that specimens of *A. rautenbachi* collected in the north-east of South Africa were netted (hence there being no information on roosts). The species account by Happold and Van Cakenberghe (2013) for *A*. cf. *helios* gave details on distribution and habitat for specimens with glands on the uropatagium and myotodont lower molars. They also referenced work for bats reported as *A. nanus*, but having *A*. cf. *helios* characters, providing information on roost, social organisation and reproduction, and limited information on echolocation, predators, and ectoparasites. Included was O'Shea's (1980) 13-month long study at a locality in Kenya south-east of Nairobi near the Galana River, which was on bats with paired glands on the uropatagium. He observed them roosting in *P. reclinata* palm leaves rather than the rolled leaves of musaceous plants as had previously been described for *A. nanus*, and reported on their social organisation and reproduction, as well as their echolocation.

Happold and Van Cakenberghe (2013) reported *A*. cf. *helios* primarily from Kenya, extending into Somalia, and Uganda, with limited distributions in Tanzania and South Sudan, and the possibility of records from Djibouti, South Africa and west Africa. The latter was based on O'Shea's observation of thatch roosting bats with glands on the tail

from Ivory Coast (Happold and Happold, 1996), and specimens with glands on the uropatagium from Cote d'Ivoire, Ghana and Nigeria (Happold and Van Cakenberghe, 2013). Not all the specimens previously reported as *A*. cf. *helios* were assessed in this study, of those that were, records of specimens now assigned to *A. rautenbachi* indicated an easterly distribution in Africa occurring in north-eastern South Africa, Mozambique and Kenya.

While their localities occurred across different vegetation types many were associated with rivers and their wetland areas. Individuals definitively identified by molecular techniques were caught in north-eastern South Africa, at two localities within the Makuleka wetlands. One was in a narrow section of Lowveld Riverine Forest (Rutherford *et al*., 2006) north of the Luvuvhu River, the other on the floodplain between the Limpopo River and the riverine forest and flood pans, in Subtropical Alluvial Vegetation (Rutherford *et al*., 2006) dominated by Graminoids and *Phoenix reclinate*. Based on morphological assignment to A. *rautenbachi* the species is also known from the riverine area of the Pungwe River running beside the Gorongoza National Park in Mozambique, and several localities in Kenya. Actual locations for some of the Kenyan locality names indicated in the records of some specimens collected in the early 1900's were difficult to locate geographically (Appendix 1). If the interpretation of spellings of older names was correct several were from different stretches of the Ewaso Ngiro River and near the Kerio River. Happold and Van Cakenberghe (2013) also reported specimens of *A*. cf. *helios* from along the Jubba and Webi Shabeele rivers in South Somalia.

Geldenhys *et al*. (2018) identified adenovirus and herpesvirus from pooled samples that included the holotype (TM 48535) and two other specimens referred to *A*. *rautenbachi* **sp. nov.** (TM 48534, 48536).

Discussion

For some time there has been confusion about the morphological characters associated with *A. helios* as named by Heller (1912). Since glands were not observed on the uropatagium of the *A. helios* holotype and the lower molar tooth morphology was nyctalodont, the name *A*. cf. *helios* had been used for individuals with a pair of glands on the uropatagium and myotodont lower molars (Happold and Van Cakenberghe, 2013). Contradicting the findings of Happold and Van Cakenberghe (2013) that *A. nanus* lower molar had the nyctalodont morphology, in this study we found *A. nanus*, *A*. cf *nanus* and *A*. *rautenbachi* lower molars primarily showed the myotodont morphology (Figure 2). Exceptions were combinations of both morphologies occurring on different teeth within the same toothrow. As tooth-wear influenced identification of these morphologies we suggest that if this character is used for identification purposes the morphology should be assessed for all the teeth in the toothrow and the degree of toothwear is considered as to whether it obscures the morphology. Based on molecular genetics, bacular and cranio-dental and other morphological characters we herein described *A. rautenbachi* the Kruger tail-gland bat to replace *A*. cf. *helios*. If Kenyan specimens with glands on the uropatagium are confirmed as *A. rautenbachi*, this common name would replace Samburu Pipistrelle (sensu Happold and Van Cakenberghe, 2013). While the molecular genetic analyses presented here included many of the sequences from Monadjem *et al*. (2021), the sequence presented here for *A. rautenbachi* was not previously represented in Monadjem *et al*. (2021).

Differentiating *A. rautenbachi* from *A. nanus* using molecular, bacula and cranio-dental analyses also revealed differences within *A. nanus*. Except for one specimen from Zimbabwe, the *A. nanus* investigated could be separated on molecular, bacula and cranio-dental characters into two groups with different geographic distributions. One group, with individuals from the eastern parts of South Africa, Eswatini and Mozambique, included cranio-dental measurements of syntypes of *A. nanus* as named by Peters (1852). The other group included individuals from northern parts of South Africa and other more north-westerly African countries (Zimbabwe, Malawi, Botswana, Namibia, Zambia, Republic of the Congo, Nigeria, Liberia, The Gambia, and Senegal). As the cranio-dental analyses of this latter group only included holotypes of two of the many *A. nanus* synonyms from the regions represented (see the ACR (2024) for the complete synonym list), and the bacula and molecular genetic analyses were not comprehensive across the countries represented, it was chosen to refer to these individuals as *A*. cf. *nanus* pending more extensive geographic investigations. The molecular genetic sequence identified here for *A*. *nanus* was not the same as any of the sequences for *A. nanus* in Monadjem *et al*. (2021). Two specimens from Botswana (TM48486 & 48488) here referred to as *A*. cf. *nanus*, were in Monadjem *et al*. (2021) in the first cluster of *A. nanus* in their Figure 3b (page 10). Given *A. helios* was only represented in this study by the holotype, it might be worth further investigation to know if the last cluster of *A. nanus* in Figure 3b (page 10) from Monadjem *et al*. (2021) with specimens from Kenya and Tanzania are *A. helios*.

An earlier intra-specific morphometric analysis of cranio-dental measurements of *A. nanus* from southern Africa identified geographic variation, albeit with no significant clinal variation in relation to latitude or longitude and had not providing any other explanation for the variation (Kearney, 2005). The PCA and cluster analysis in Kearney (2005) revealed the same pattern as reported above with regards the differences between *A. nanus* and *A*. cf. *nanus*, with similar measurements loading most highly (width across the canines, braincase width and length of the first upper molar tooth). However, in the absence of additional molecular genetic information and measurements of the bacula the cranio-dental distinctions reported here between *A. nanus* and *A*. cf. *nanus* were not recognised in Kearney (2005).

Given all individuals in the genetically identified series of *A. rautenbachi* had a pair of glands on the uropatagium on either side of the tail, whereas none of the individuals of *A. nanus* and *A*. cf. *nanus* clade 1 or clade 2 that were assessed, and the holotype of *A. helios* had no glands on the uropatagium, this appears to be a good morphological characteristic to identify *A. rautenbachi*. However, further investigation is needed to assess the variability of this character, especially for the species in Kenya, given five specimens previously identified as *A. helios* from four localities in Kenya had only one gland present on the uropatagium. Although where specimens, previously identified as *A. helios,* were present at three of these localities, other individuals did have two glands present.

As previously indicated by Goodman *et al*. (2017) this is yet another example where the subtle morphological variation in vesper bats required multiple data sets, and in particular genetic data, to distinguish differences. Further work, following the integrated approach incorporating different character sets is still needed to extend the number of genetically identified individuals, as well as incorporate bio-acoustic information, and resolve the actual distribution of the species.

While the genetically identified series of *A. rautenbachi* has a small distribution from two localities in the northern-eastern part of South Africa, identification of individuals as this species by other characteristics associated with the genetically identified series in relation to cranio-dental morphology and glands on the tail indicates a more extensive distribution in Mozambique and Kenya. While the distribution of *A. rautenbachi* remains unresolved, based on the extent of these records, we recommend that *A. rautenbachi* be given the IUCN conservation status of 'Least Concern'. Although, with increased human-related transformation of large rivers, which this species appears to be associated with, the species may be of conservation concern in the near future.

Acknowledgments

We are grateful to Chris Roche (Wilderness Safaris) for initiating and supporting the bat collecting in the Makuleka Contract Park. We thank Walter Jubber (Wilderness Safaris) who understood our requirements and found us excellent netting sites. We also acknowledged the contribution of Dawn Cory-Toussaint, Louis Nel, Mike Pierce, Ernest Seamark and Jacqueline Weyer for assistance in the field. Meredith Happold is thanked for generously providing so much useful information about bats, in particular alerting us to be on the lookout for small vesper bats with tail glands. For access to specimens in various collections we thank the following curators and staff: Llyod Wingate and Fred Kigozi (Amathole Museum, Qonce), Paul Bates (Harrison Zoological Museum, Sevenoaks), Hendrik Turni (Natural History Museum, Berlin), Robert Portela-Miguez (Natural History Museum, London), Katrin Krohmann (Senckenberg Museum, Frankfurt), and Guin Zambatis (Skukuza Biological Reference Collection, Kruger National Park). Don Wilson (Smithsonian Institution, Washington) kindly provided measurements and images of the *A. helios* holotype. National Research Foundation (NRF) of South Africa grants awarded to TK facilitated travel to overseas museums to measure type specimens (grant numbers FA2005041/00002 and 2075460). The molecular work presented here was based on research supported by the South African Research Chair initiative of the Department of Science and Innovation and the National Research Foundation (NRF) of South Africa awarded to WM (grant number 98339/0219114353). The NRF is also thanked for funding the equipment based at the DNA Sanger sequencing facility in the Faculty of Natural and Agricultural Sciences, University of Pretoria (UID:78566) that was used to generate Sanger sequencing data presented in this work. The financial assistance of the National Research Foundation (NRF) towards this research is hereby acknowledged. Opinions expressed and conclusions arrived at, are those of the authors and are not necessarily to be attributed to the NRF. The publication was additionally supported by an agreement with Cornell University, under Prime Agreement 1378199 from the Burroughs Wellcome Fund, which funds the salary for MdV. Any opinions, findings, and conclusions or recommendations expressed in

this publication are those of the author(s) and do not necessarily reflect the views of Cornell University nor those of the Sponsor. For comments and corrections on earlier versions of this paper, we are grateful to the editor, and Ara Monadjem and an anonymous reviewer.

References

ACR (2024) *African Chiroptera Report. 2024*. African Bats NPC, Pretoria, xv + 1397 pp. https://doi.org/10.13140/RG.2.2.15903.27045

Benda, P., Uvizl, M., Šklíba, J., Mazoch, V. & Červený, J. (2022) African bats in the collection of the National Museum, Prague (Chiroptera). I. Bats from Zambia. *Lynx, series nova*, 53 (1), 291–323. https://doi.org/10.37520/lynx.2022.021

Bickham, J.W., Wood, C.C. & Patton, J.C. (1995) Biogeographic implications of cytochrome *b* sequences and allozymes in sockeye (*Oncorhynchus nerka*). *Journal of Heredity*, 86, 140–144. https://doi.org/10.1093/oxfordjournals.jhered.a111544

Bickham, J.W., Patton, J.C., Schlitter, D.A., Rautenbach, I.L. & Honeycutt, R.L. (2004) Molecular phylogenetics, karyotypic diversity, and partition of the genus *Myotis* (Chiroptera, Vespertilionidae). *Molecular Phylogenetics and Evolution*, 33 (2), 333–338. https://doi.org/10.1016/j.ympev.2004.06.012

Darriba, D., Taboada, G.L., Doallo, R. & Posada, D. (2012) JModelTest 2: more models, new heuristics and parallel computing. *Nature Methods*, 9, 772. https://doi.org/10.1038/nmeth.2109

Demos, T.C., Webala, P.W., Monadjem, A. & Patterson, B.D. (2025) Nuclear introns support the subtribe Laephotina and recently proposed genera of African Vespertilionidae. *Acta Chiropterologica*, 26 (2), 143–152. https://doi.org/10.3161/15081109ACC2024.26.2.001

Drummond, A.J. & Rambaut, A. (2007) BEAST: Bayesian evolutionary analysis by sampling trees. *BMC Evolutionary Biology*, 7, 214. https://doi.org/10.1186/1471-2148-7-214

Folmer, O., Black, M., Hoeh, W., Lutz, R. & Vrijenhoek, R. (1994) DNA primers for amplification of mitochondrial cytochrome *c* oxidase subunit I from diverse metazoan invertebrates. *Molecular Marine Biology and Biotechnology*, 3, 294–299.

Geldenhuys, M., Mortlock, M., Weyer, J., Bezuidt, O., Seamark, E.C., Kearney, T., Gleasner, C., Erikkil, T.H., Cui, H. & Markotter, W. (2018) A metagenomic viral discovery approach identifies potential zoonotic and novel mammalian viruses in *Neoromicia* bats within South Africa. *PloS ONE*, 13 (3), e0194527. https://doi.org/10.1371/journal.pone.0194527

Goodman, S.M., Rakotondramananus, C.F., Ramasindrazana, B., Kearney, T., Monadjem, A., Schoeman, M.C., Taylor, P.J., Naughton, K. & Appleton, B. (2015) An integrative approach to characterize Malagasy bats of the subfamily Vespertilioninae. *Zoological Journal of the Linnean Society*, 173 (4), 988–1018. https://doi.org/10.1111/zoj.12223

Goodman, S.M., Kearney, T., Ratsimbazafy, M.M. & Hassanin, A. (2017) Description of a new species of *Neoromicia* (Chiroptera: Vespertilionidae) from southern Africa: a name for '*N.* cf. *melckorum'*. *Zootaxa*, 4236 (2), 351–374. https://doi.org/10.11646/zootaxa.4236.2.10

Hall, T.A. (1999) BioEdit: a user-friendly biological sequence alignment editor and analysis program for Windows 95/98/NT. *Nucleic Acids Symposium Series*, 41, 95–98.

Hammer, O., Harper, D.A.T. & Ryan, P.D. (2001) PAST: Paleontological Statistics software package for education and data analysis. *Palaeontologia Electronica*, 4 (1), 1–9.

Happold, D.C.D. & Happold, M. (1996) The social organization and population dynamics of leaf-roosting banana bats, *Pipistrellus nanus* (Chiroptera, Vespertilionidae), in Malawi, east-central Africa. *Mammalia*, 60 (4), 517–544. https://doi.org/10.1515/mamm.1996.60.4.517

Happold, M. & Van Cakenberghe, V. (2013) *Pipistrellus* cf. *helios* Samburu Pipistrelle. *In*: Happold, M. & Happold, D.C.D. (Eds.), *Mammals of Africa. Vol. IV. Hedgehogs, Shrews and Bats*. Bloomsbury Publishing, London, pp. 627–629.

Harima, H., Qiu, Y., Yamagishi, J., Kajihara, M., Changula, K., Okuya, K., Isono, M., Yamaguchi, T., Ogawa, H., Nao, N., Sasaki, M., Simulundu, E., Mweene, A.S., Sawa, H., Ishihara, K., Hang'ombe, B.M. & Takada, A. (2023) Surveillance, Isolation, and Genetic Characterization of Bat Herpesviruses in Zambia. *Viruses*, 15 (6), 1369. https://doi.org/10.3390/v15061369

Hassanin, A., Colombo, R., Gembu, G.-C., Merle, M., Tu, V.T., Gorfol, T., Akawa, P.M., Csorba, G., Kearney, T., Monadjem, A. & Ing, R.K. (2017) Multilocus phylogeny and species delimitation within the genus *Glauconycteris* (Chiroptera, Vespertilionidae), with the description of a new bat species from the Tshopo Province of the Democratic Republic of the Congo. *Journal of Zoological Systematics and Evolutionary Research*, 56, 1–22. https://doi.org/10.1111/jzs.12176

Hassanin, A., Delsuc, F., Ropiquet, A., Hammer, C., Jansen van Vuuren, B., Matthee, C., Ruiz-Garcia, M., Catzeflis, F., Areskoug,

V., Nguyen, T.T. & Couloux, A. (2012) Pattern and timing of diversification of Cetartiodactyla (Mammalia, Laurasiatheria), as revealed by by a comprehensive analysis of mitochondrial genomes. *Comptes Rendus Biologies*, 335, 32–50. https://doi.org/10.1016/j.crvi.2011.11.002

Hill, J.E. & Harrison, D.L. (1987) The baculum in the Vespertilioninae (Chiroptera: Vespertilionidae) with a systematic review, a synopsis of *Pipistrellus* and *Eptesicus*, and the descriptions of a new genus and subgenus. *Bulletin of the British Museum (Natural History), Zoology Series*, 52 (7), 225–305.

Heller, E. (1912) New races of insectivores, bats and lemurs from British East Africa. *Smithsonian Miscellaneous Collections*, 60 (12), 1–13.

Kearney, T.C. (2005) *Systematic revision of southern African species in the genera Eptesicus, Neoromicia, Hypsugo and Pipistrellus (Chiroptera: Vespertilionidae).* Ph.D. Thesis, The University of KwaZulu-Natal, Durban, 580 pp.

Kearney, T.C. & Taylor, P.J. (2011) Selection of cranial and mandible measurements for traditional morphometric analyses of southern African vesper bats of the genera *Eptesicus*, *Hypsugo*, *Neoromicia* and *Pipistrellus* (Mammalia: Chiroptera: Vespertilionidae). *Annals of the Ditsong National Museum of Natural History*, 1, 53–61.
https://hdl.handle.net/10520/EJC83700

Kearney, T.C., Volleth, M., Contrafatto, G. & Taylor, P.J. (2002) Systematic implications of chromosome GTG-band and bacula morphology for Southern African Eptesicus and Pipistrellus and several other species of Vespertilioninae (Chiroptera: Vespertilionidae). *Acta Chiropterologica*, 4 (1), 55–76. https://doi.org/10.3161/001.004.0107

Koopman, K.F. (1993) Order Chiroptera. *In*: Wilson, D.E. & Reeder, D.M. (Eds.), *Mammal species of the world: a taxonomic and geographic reference*. Smithsonian Institution Press, Washington, D.C., pp. 137–241.

Kumar, S., Stecher, G., Li, M., Knyaz, C. & Tamura, K. (2018) MEGA X: molecular evolutionary genetics analysis across platforms. *Molecular Biology and Evolution*, 35, 1547–1549. https://doi.org/10.1093/molbev/msy096

LaVal, R.K. & LaVal, M.L. (1977) Reproduction and behaviour of the African Banana Bat, *Pipistrellus nanus*. *Journal Of Mammalogy*, 58 (3), 403–410. https://doi.org/10.2307/1379339

Meester, J.A.J., Rautenbach, I.L., Dippenaar, N.J. & Baker, C.M. (1986) *Classification of Southern African mammals. Transvaal Museum Monograph. No. 5*. Transvaal Museum, Pretoria, 359 pp.

Miller, M.A., Pfeiffer, W. & Schwartz, T. (2010) Creating the CIPRES Science Gateway for inference of large phylogenetic trees. *In*: *2010 Gateway Computing Environments workshop (GCE)*. IEEE, New Orleans, Louisiana, pp. 1–8. https://doi.org/10.1109/GCE.2010.5676129

Monadjem, A., Richards, L., Taylor, P.J. & Stoffberg, S. (2013) High diversity of pipistrelloid bats (Vespertilionidae: *Hypsugo*, *Neoromicia* and *Pipistrellus*) in a West African rainforest with the description of a new species. *Zoological Journal of the Linnean Society*, 167 (1), 191–207. https://doi.org/10.1111/j.1096-3642.2012.00871

Monadjem, A., Demos, T.C., Dalton, D.L., Webala, P.W., Musila, S., Kerbis Peterhans, J.C. & Patterson, B.D. (2021) A revision of pipistrelle-like bats (Mammalia: Chiroptera: Vespertilionidae) in East Africa with the description of new genera and species. *Zoological Journal of the Linnean Society*, 191 (4), 1114–1146. https://doi.org/10.1093/zoolinnean/zlaa087

O'Shea, T.J. (1980) Roosting, social organization and the annual cycle in a Kenya population of the bat *Pipistrellus nanus*. *Zeitschrift für Tierpsychologie*, 53 (2), 171–195. https://doi.org/10.1111/j.1439-0310.1980.tb01048.x

Peters, W.C. (1852) *Naturwissenschaftliche Reise nach Mossambique: 1. Säugethiere. Mit sechs und vierzig Taflen. Zoologie*. Druck und Verlag von Georg Reimer, 670 pp.

Rautenbach, I.L., Fenton, M.B. & Braack, L.E.O. (1985) First records of five species of insectivorous bats from the Kruger National Park. *Koedoe*, 28, 73–80. https://doi.org/10.4102/koedoe.v28i1.537

Rautenbach, I.L., Fenton, M.B. & Whiting, M.J. (1996) Bats in riverine forests and woodlands: a latitudinal transect in southern Africa. *Canadian Journal of Zoology*, 74, 312–322. https://doi.org/10.1139/z96-039

Rosevear, D.R. (1965) *The bats of West Africa.* British Museum (Natural History), London, 418 pp.

Rutherford, M.C., Mucina, L. & Powrie, L.W. (2006) Biomes and bioregions of southern Africa. *The vegetation of South Africa, Lesotho and Swaziland,* 19, 30–51.

Simmons, N.B. (2005) Order Chiroptera. *In*: Wilson, D.E. & Reeder, D.M. (Eds.), *Mammal species of the world: a taxonomic and geographic reference*. John Hopkins University Press, Baltimore, Maryland, pp. 312–529.

Torrent, L., Juste, J., Garin, I., Aihartza, J., Dalton, D.L., Mamba, M., Tanshi, I., Powell, L.L., Padidar, S., Garcia Mudarra, J.L., Richards, L. & Monadjem, A. (2025) Taxonomic revision of African pipistrelle-like bats with a new species from the West Congolean rainforest. *Zoological Journal of the Linnean Society*, 204 (2), zlaf020. https://doi.org/10.1093/zoolinnean/zlaf020

APPENDIX 1. Museum numbers and locality information for specimens of *Afronycteris* used in this study. Individuals identified as *A.* cf. *nanus* reflect differences found within *A. nanus*. The museum acronyms are described in the materials and methods section. Their individual uses are indicated for sequences based on Cytb, COI and 12S with associated GenBank numbers, and other data (1 = craniodental, 2 = external, and 3 = baculum measurements, 4 = uropatagium viewed for glands, and 5 = observation of the lower molar nyctalodont / myotodont cusp pattern). ? = no further information available. * = bacula reported in Hill and Harrison (1987). ** = sequences previously reported in Goodman *et al*. (2015).

Species	Museum number	Locality	Y	X	Cytb	COI	12S	Other data
Afronycteris **sp. nov.**	NHMUK 1912.7.1.22	Kenya: Ndolo	ca. -1.8410	ca. 37.404				1,5
Afronycteris **sp. nov.**	NHMUK 1911.12.1.4	Kenya: Nyama Nyango, Eusso Nyiro	ca. 0.78075	ca. 38.08211				1,5
Afronycteris **sp. nov.**	NHMUK 1912.7.1.24	Kenya: Soriau/Soriqu	?	?				1,4,5
Afronycteris **sp. nov.**?	NHMUK 1912.7.1.25	Kenya: Soriau/Soriqu	?	?				1,4,5
Afronycteris **sp. nov.**	NHMUK 1912.7.1.27	Kenya: [Eusso Nyiro] Ewaso Ngiro River	ca. 0.78075	ca. 38.08211				1,4,5
Afronycteris **sp. nov.**	NHMUK 1912.7.1.29	Kenya: [Eusso Nyiro] Ewaso Ngiro River	ca. 0.78075	ca. 38.08211				1,4,5
Afronycteris **sp. nov.**	NHMUK 1912.7.1.30	Kenya: [Eusso Nyiro] Ewaso Ngiro River	ca. 0.78075	ca. 38.08211				1,4,5
Afronycteris **sp. nov.**	NHMUK 1912.7.1.31	Kenya: Chanler Falls, Ewaso Ngiro River	0.78075	38.08211				1,4,5
Afronycteris **sp. nov.**	NHMUK 1969.207	Kenya: S Turkana, Kangatet	ca. 2.2513	ca. 36.1679				1,3*,4,5
Afronycteris **sp. nov.**	NHMUK 1975.2556	Kenya: Isiolo, Samburu lodge	0.566667	37.583333				1,4,5
Afronycteris **sp. nov.**	NHMUK 1912.7.1.28	Kenya: [Eusso Nyiro] Ewaso Ngiro River	ca. 0.78075	ca. 38.08211				1,4,5
Afronycteris **sp. nov.**	NHMUK 1912.7.1.26	Kenya: Soriau/Soriqu	?	?				1,4,5
Afronycteris **sp. nov.**	NHMUK 1912.7.1.32	Kenya: Chanler Falls, Ewaso Ngiro River	0.78075	38.08211				1,4
Afronycteris **sp. nov.**?	NHMUK 1911.12.1.3	Kenya: Chanler Falls, Ewaso Ngiro River	0.78075	38.08211				1,5
Afronycteris **sp. nov.**	NHMUK 1939.133	Kenya: [N. Guaso/Eusso Nyiro] N. Ewaso Ngiro River	ca. 0.78075	ca. 38.08211				3*,4
Afronycteris **sp. nov.**	HZM 1.4085	Kenya: Archer's Post	0.566667	37.583333				1,2,4
Afronycteris **sp. nov.**	HZM 2.4086	Kenya: Archer's Post	0.566667	37.583333				2,3*,4
Afronycteris **sp. nov.**	HZM 3.4087	Kenya: Archer's Post	0.566667	37.583333				1,2,4
Afronycteris **sp. nov.**	HZM 4.4088	Kenya: Archer's Post	0.566667	37.583333				1,2,4
Afronycteris **sp. nov.**	TM 50951	Mozambique: Gorongoza NP	-19.05872	34.22744				1,2,4,5
Afronycteris **sp. nov.**	TM 51005	Mozambique: Vinho village, Pungue river	-18.994972	34.351				2,4
Afronycteris **sp. nov.**	CHIR-KNP-UP-921	South Africa: KNP, Makuleka Contract Park	-22.42151	31.2238	PX103072		PX105508	1,2,4
Afronycteris **sp. nov.**	TM 48535	South Africa: KNP, Makuleka Contract Park	-22.34657	31.11595	PX103059	PX103240	PX105500	1,2,3,4,5
Afronycteris **sp. nov.**	TM 48536	South Africa: KNP, Makuleka Contract Park	-22.34657	31.11595	PX103064		PX105506	4,5
Afronycteris **sp. nov.**	TM 48537	South Africa: KNP, Makuleka Contract Park	-22.34657	31.11595	PX103065		PX105507	1,2,4,5

.....continued on the next page

APPENDIX 1. (Continued)

Species	Museum number	Locality	Y	X	Cytb	COI	12S	Other data
Afronycteris **sp. nov.**	TM 48587	South Africa: KNP, Makuleka Contract Park	-22.34657	31.11595	PX103068		PX105512	1,2,4,5
A. cf. *nanus*	TM 50953	Botswana: Vumbura Plains	-19.00688	22.92771				1,2,4
A. cf. *nanus*	TM 50954	Botswana: Vumbura Plains	-19.00688	22.92771				1,2,4
A. cf. *nanus*	TM 50955	Botswana: Kwetsani Island	-19.24625	22.53737				1,2,4
A. cf. *nanus*	TM 50956	Botswana: Kwetsani Island	-19.24625	22.53737				1,2
A. cf. *nanus*	TM 50952	Botswana: Vumbura Plains	-19.00919	22.92732				1,2,4
A. cf. *nanus*	TM 48486	Botswana: Chitabe, Gomoti River	-19.00688	22.92771	**			1,3,4,5
A. cf. *nanus*	TM 48488	Botswana: Vumbura Plains	-19.00688	22.92771	**			1,3,4,5
A. cf. *nanus*	HZM 1.4024	Liberia: Nr. Monrovia	6.310556	-10.804722				1,2
A. cf. *nanus*	HZM 2.4025	Liberia: Nr. Monrovia	6.310556	-10.804722				1,2
A. cf. *nanus*	HZM 3.4026	Liberia: Nr. Monrovia	6.310556	-10.804722				1,2
A. cf. *nanus*	HZM 4.4027	Liberia: Nr. Monrovia	6.310556	-10.804722				1,2
A. cf. *nanus*	ZMB 4729	Liberia: ?	?	?				1
A. cf. *nanus*	AM 1903	Malawi: Chiromo	-16.55	35.133333				1
A. cf. *nanus*	NHMUK 1925.12.4.20	Namibia: NW Ovamboland, Ukualukasi	-17.32	14.616667				1
A. cf. *nanus*	AM 1902	Namibia: SE Rundu	-18.1	20.38				1
A. cf. *nanus*	NHMUK 1911.3.24.4	Nigeria: Bauchi Province, Kabir	8.4	9.566667				1
A. cf. *nanus*	NHMUK 1921.2.11.8	Nigeria: Kano	11.996389	8.516667				1
A. cf. *nanus*	HZM 1.2771	Nigeria: Sokoto	13.033333	5.25				1,2
A. cf. *nanus*	HZM 2.2772	Nigeria: Sokoto	13.033333	5.25				1,2
A. cf. *nanus*	HZM 3.2778	Nigeria: Sokoto	13.033333	5.25				1,2
A. cf. *nanus*	SMF 93321	Republic of the Congo: Bateke-Plateau, ca 30 km E Kinshasa	-3.500833	15.7483333				1
A. cf. *nanus*	SMF 92761	Senegal: Niokolo-Koba NP, Lengue Kountou	13.033333	-13.066667				1,2
A. cf. *nanus*	CHIR KNP 95	South Africa: KNP, Letaba	-23.833889	31.633333				1
A. cf. *nanus*	TM 34212	South Africa: KNP, Pafuri	-22.433333	31.183333				1,5
A. cf. *nanus*	TM 34223	South Africa: KNP, Pafuri	-22.433333	31.183333				1,5
A. cf. *nanus*	TM 37816	South Africa: KNP, Pafuri	-22.425	31.3				1,5
A. cf. *nanus*	TM 38604	South Africa: KNP, Pafuri	-22.416667	31.3				1,5
A. cf. *nanus*	TM 47133	South Africa: Limpopo, Phalaborwa	-24.05	31.05				1,2,4,5

.....continued on the next page

APPENDIX 1. (Continued)

Species	Museum number	Locality	Y	X	Cytb	COI	12S	Other data
A. cf. *nanus*	TM 47143	South Africa: KNP, Pafuri	-22.416667	31.25				1,5
A. cf. *nanus*	TM 48505	South Africa: KNP, Pafuri	-22.42151	31.2238	PX103060		PX105501	1,2,4,5
A. cf. *nanus*	TM 48508	South Africa: KNP, Pafuri	-22.42151	31.2238	PX103061		PX105502	1,2,4,5
A. cf. *nanus*	TM 48509	South Africa: KNP, Pafuri	-22.42151	31.2238	PX103062		PX105503	1,2,4,5
A. cf. *nanus*	TM 48533	South Africa: KNP, Pafuri	-22.34657	31.11595	PX103063		PX105504	1,2,3,4,5
A. cf. *nanus*	TM 48534	South Africa: KNP, Pafuri	-22.34657	31.11595	PX103071		PX105505	1,2,4,5
A. cf. *nanus*	TM 48571	South Africa: KNP, Pafuri	-22.42151	31.2238				1,2,4
A. cf. *nanus*	TM 48572	South Africa: KNP, Pafuri	-22.42151	31.2238	PX103073	PX103242	PX105509	1,2,4
A. cf. *nanus*	TM 48573	South Africa: KNP, Pafuri	-22.42151	31.2238	PX103066	PX103243	PX105510	1,2,3,4,5
A. cf. *nanus*	TM 48578	South Africa: KNP, Pafuri	-22.42601	31.29873	PX103067	PX103244	PX105511	1,2,4,5
A. cf. *nanus*	TM 48597	South Africa: KNP, Pafuri	-22.34657	31.11595	PX103069		PX105513	1,2,4
A. cf. *nanus*	SMF 91.077	The Gambia: NW Lamin, Abuko NR	13.391389	-16.6525				1,2
A. cf. *nanus*	SMF 91.078	The Gambia: NW Lamin, Abuko NR	13.391389	-16.6525				1,2
A. cf. *nanus*	SMF 91.079	The Gambia: NW Lamin, Abuko NR	13.391389	-16.6525				1,2
A. cf. *nanus*	SMF 91.080	The Gambia: NW Lamin, Abuko NR	13.391389	-16.6525				1,2
A. cf. *nanus*	NMZL-ECJS-15/2008	Zambia: Kafue NP, Lafupa	-14.615590	26.190830				1,2
A. cf. *nanus*	NMZL-ECJS-54/2008	Zambia: Kafue NP, Lafupa	-14.617350	26.191700				1,2
A. cf. *nanus*	NMZL-ECJS-60/2008	Zambia: Kafue NP, Lafupa	-14.616800	26.190960				1,2
A. cf. *nanus*	NMZL-ECJS-9/2008	Zambia: Kafue NP, Lafupa	-14.614300	26.188400				1,2
A. cf. *nanus*	DM 5366	Zimbabwe: Eastern highlands, Chingamwe Estate	-18.45	32.75				1,2,3
A. cf. *nanus*	TM 34607	Zimbabwe: Mount Silinda, Chirinda Forest	-20.4	32.7				1,5
A. cf. *nanus*	TM 34769	Zimbabwe: Rusito Forest	-20.033333	32.983333				1,5
A. cf. *nanus*	TM 34782	Zimbabwe: Rusito Forest	-20.033333	32.983333				3,5
A. cf. *nanus*	TM 34783	Zimbabwe: Rusito Forest	-20.033333	32.983333				1,5
A. cf. *nanus*	TM 34973	Zimbabwe: Sengwa Wildlife Research Station	-18.166667	28.216667				1,5
A. cf. *nanus*	TM 41618	Zimbabwe: Sentinal Ranch	-22.166667	29.5				1,5
A. cf. *nanus*	TM 41621	Zimbabwe: Sentinal Ranch	-22.166667	29.5				1,5
A. cf. *nanus*	TM 41622	Zimbabwe: Sentinal Ranch	-22.166667	29.5				1,5

.....continued on the next page

APPENDIX 1. (Continued)

Species	Museum number	Locality	Y	X	Cytb	COI	12S	Other data
A. helios	USNM 181813	Kenya: 48 km S Mt Marsabit, Merelle Water	1.383333	37.733333				1,2,4
A. nanus	ZMB 588c	Mozambique: Inhambane	-23.865	35.383333				1
A. nanus	ZMB 588a	Mozambique: Inhambane	-23.865	35.383333				1
A. nanus	CHIR KNP 37	South Africa: KNP, Skukuza	-24.994722	31.590278				1
A. nanus	CHIR KNP 38	South Africa: KNP, Skukuza	-24.994722	31.590278				1
A. nanus	CHIR KNP 39	South Africa: KNP, Skukuza	-24.994722	31.590278				1
A. nanus	CHIR KNP 40A	South Africa: KNP, Pretoriuskop	-25.166667	31.265833				1
A. nanus	DM 5365	South Africa: Renishaw	-30.26667	30.733333				1,2,3
A. nanus	DM 5367	South Africa: Jozini Dam	-27.416667	32.066667				1,2,3
A. nanus	DM 5402	South Africa: Renishaw	-30.266667	30.733333				1,2,3
A. nanus	DM 5404	South Africa: Renishaw	-30.266667	30.733333				1,2,3
A. nanus	DM 5869	South Africa: Stainbank NR	-29.9	30.933333				1,2,3
A. nanus	DM 5870	South Africa: Stainbank NR	-29.9	30.933333				1,2,3
A. nanus	DM 5871	South Africa: Stainbank NR	-29.9	30.933333				1,2,3
A. nanus	DM 5900	South Africa: Ithala GR	-27.541667	31.373056				1,2,3
A. nanus	DM 5901	South Africa: Ithala GR	-27.541667	31.373056				1,2,3
A. nanus	TM 1076	South Africa: Port St Johns	-31.633333	29.55				1
A. nanus	TM 35284	South Africa: Mkuzi GR	-27.783333	32.2				1,5
A. nanus	TM 35285	South Africa: Mkuzi GR	-27.783333	32.2				1,5
A. nanus	TM 35288	South Africa: Mkuzi GR	-27.783333	32.2				1,5
A. nanus	TM 35289	South Africa: Mkuzi GR	-27.783333	32.2				1,5
A. nanus	TM 39817	South Africa: Ngome FR	-27.833333	31.4125				1,5
A. nanus	TM 41999	South Africa: KNP, Bobomene	-22.416667	31.2				1,5
A. nanus	TM 43269	South Africa: Bothas Hill	-29.75	30.733333				1,5
A. nanus	TM 46480	South Africa: Mpumalanga, Blyde River Canyon NR	-24.666667	30.8				1,3,5
A. nanus	TM 49146	South Africa: Ga Mafefe	-24.144022	30.1169	PX103070	PX103241	PX105514	1,2,3,4,5
A. nanus	TM 39137	South Africa: Ngome FR	-27.833333	31.4125				1,5
A. nanus	DM 5879	Eswatini: 10 km N Simunye	-26.116667	31.95				3
A. nanus	DM 5880	Eswatini: 10 km N Simunye	-26.116667	31.95				1,2
A. nanus	TM 34609	Zimbabwe: Mount Silinda, Chirinda Forest	-20.4	32.7				1,5

Supplementary Materials. Four files are available on figshare. Supplementary Information (https://doi.org/10.6084/m9.figshare.30999094).—MS Excel spreadsheet containing pairwise distance of the Cytb, COI, and 12S markers; and Figures of Bayesian phylogenetic analyses based on COI and 12S rRNA, and a PCA of eight skull measurements.

Table S1: Percentage Estimates of Evolutionary Divergence between the Cytb Nucleotide Sequences of *Afronycteris* included in the analyses.

Table S2: Percentage Estimates of Evolutionary Divergence between the COI Nucleotide Sequences of *Afronycteris* included in the analyses.

Table S3: Percentage Estimates of Evolutionary Divergence between the 12S Nucleotide Sequences of *Afronycteris* included in the analyses.

Figure S1: Bayesian phylogenetic analysis based on cytochrome c oxidase subunit 1 (COI) sequences (618nt) from species in the Vespertilionidae family (TPM2uf+I+G substitution model based on the Bayesian information criterion (BIC)). Genera are indicated at internal branching points. The phylogenetic position of *Afronycteris* **sp. nov.** is indicated in red, other *Afronycteris* sequences generated in this study from specimens collected in the northern part of South Africa are indicated in blue and representative sequences from literature is represented in black. Museum numbers of specimens from which sequences were generated are indicated in brackets. The Bayesian phylogeny was constructed using BEAST v2.6.6. Only posterior probabilities of >0.5 are indicated.

Figure S2: Bayesian phylogenetic analysis based on 12S rRNA (12S) sequences (872nt) from species in the Vespertilionidae family (TIM2+I+G substitution model based on the Bayesian information criterion (BIC)). Genera are indicated at internal branching points. The phylogenetic position of *Afronycteris* **sp. nov.** is indicated in red, other *Afronycteris* sequences generated in this study from specimens collected in the northern part of South Africa are indicated in blue and representative sequences from literature is represented in black. Museum numbers of specimens from which sequences were generated are indicated in brackets. The Bayesian phylogeny was constructed using BEAST v2.6.6. Only posterior probabilities of >0.5 are indicated.

Figure S3: Plot of first two principal components based on variance-covariance coefficients of eight skull measurements from 104 specimens of *Afronycteris* **sp. nov.** (filled circles), *A. rautenbachi* **sp. nov.**—BMNH 1912.7.1.26 and 1912.7.1.32 (open circles), *A. helios* (filled triangle), *A. nanus* (open square) and *A.* cf. *nanus* (open triangle). Symbols of individuals that were sequenced with Cytb are the same colour as clades identified in Figure 3. Holotypes are identified as follows: a = *Pipistrellus nanus australis* Roberts 1913 (TM 1076), c = *Pipistrellus culex* Thomas, 1911 (NHMUK 1911.3.24.4), f = *Pipistrellus fouriei* Thomas, 1926 (NHMUK 1925.12.4.20), and h = *Pipistrellus helios* Heller, 1912 (USNM 181813). Syntypes of *Vespertilio nanus* Peters, 1852 (ZMB 588a and ZMB 588c) are identified by an 'n'.